Large bubble entrapment due to a falling drop on a liquid surface

Gautam Biswas
J C Bose National Fellow

Indian Institute of Technology Guwahati, Guwahati-781039

IMPACT OF LIQUID DROP ON LIQUID AND SOLID

SPLASHING

COALESCENCE

HYDROPHILIC

HYDROPHOBIC

Impact of drop on liquid

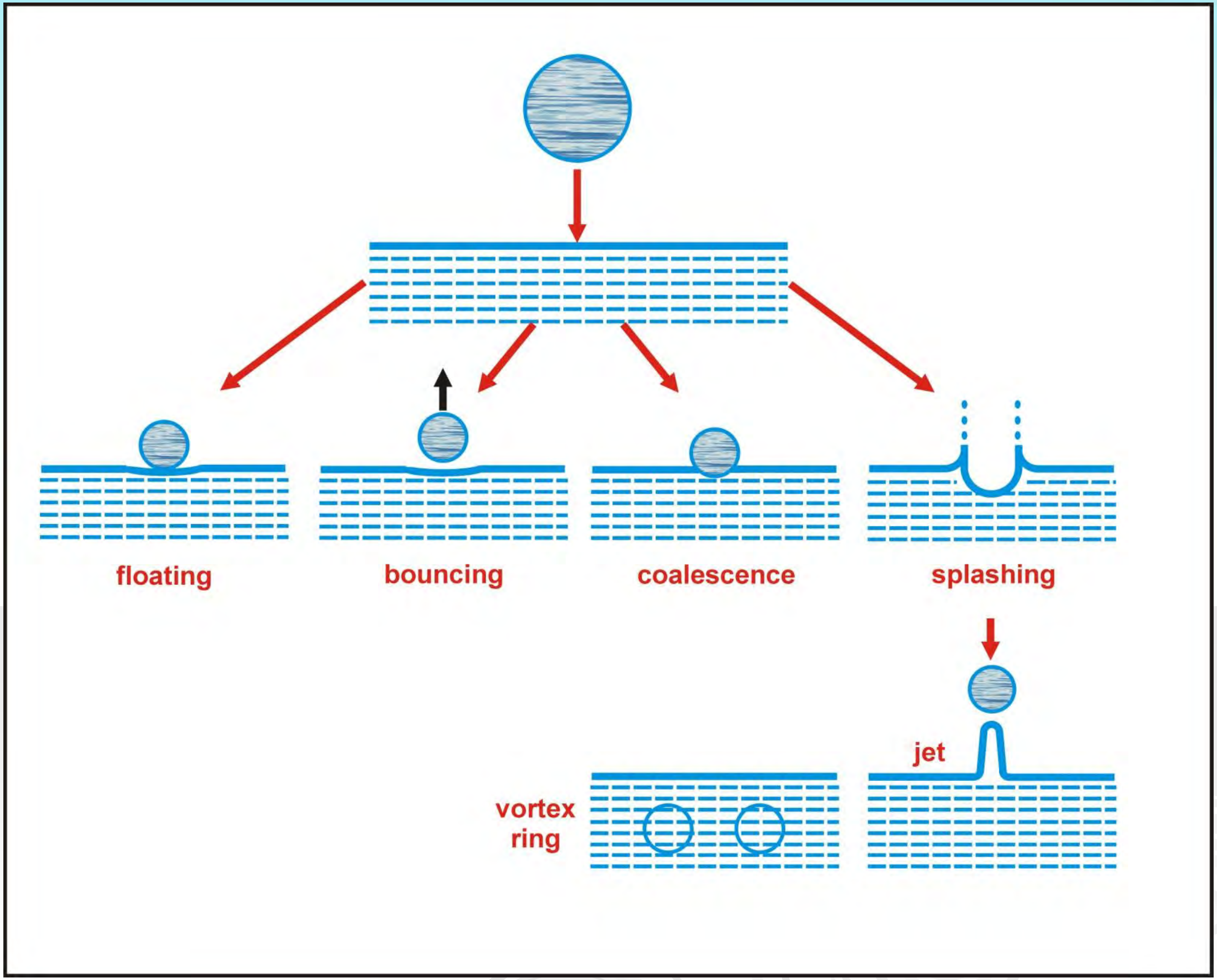

CLSVOF method (Computational domain)

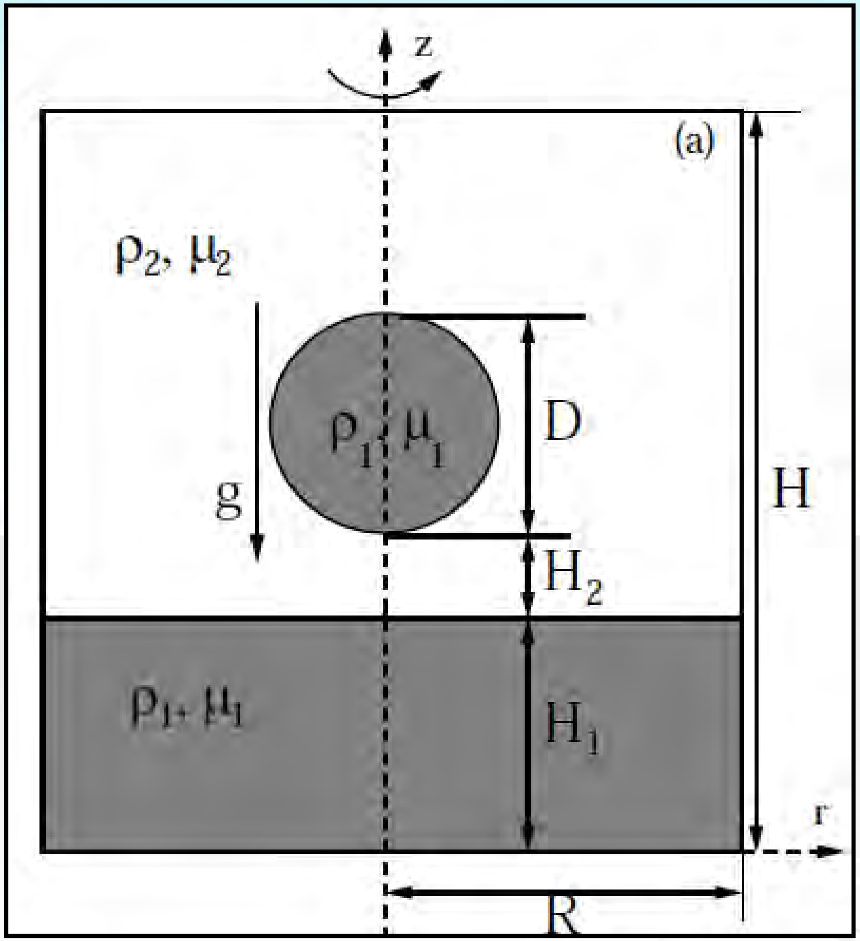

Nondimensional parameters (liquid/liquid system):

$$Oh_1 = \mu_1 \Big/ \sqrt{\rho_m \sigma D},$$

$$Oh_2 = \mu_2 \Big/ \sqrt{\rho_m \sigma D},$$

$$Bo = \rho_c D^2 g \Big/ \sigma,$$

$$A = \rho_c \Big/ 2\rho_m$$

➢ Volume of Fluid (VOF) (Hirt and Nichols (1979))

- The method tracks volume fraction of each fluid in cells that contains portions of the interface, rather then the interface itself.

- Variable: liquid void fraction,

$$\alpha = \frac{\rho - \rho_g}{\rho_l - \rho_g}$$

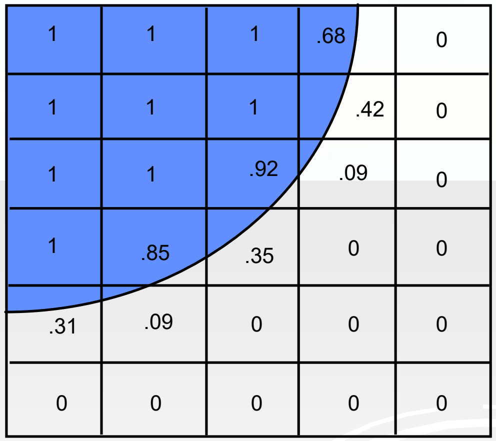

$\alpha = 0$ gas

$\alpha = 1$ Liquid

$0 < \alpha < 1$ A two phase cell

Volume of Fluid Continued…

- At each time step interface is reconstructed solving advection equation (geometrically)
- Update the void fractions for next time step

Advantages

- Liquid - gas interface is captured explicitly
- Satisfies mass conservation

Disadvantages

- Not very accurate for flows with high density differences

Level set (LS) (Osher and Sethian (1988))

ϕ

- Interface is represented by a smooth level set function

$$\phi(\vec{r},t)\begin{cases} <0 \text{ in the fluid 1 region} \\ =0 \text{ at the interface} \\ >0 \text{ in the fluid 2 region} \end{cases}$$

Advantages

- The level set function varies smoothly across the interface: gives accurate **curvature** and interface **normal vector**.

Disadvantages

- When interface is advected parallel, it gives accurate result. But for deforming interface there is mass loss.

Interface Construction

- **SLIC (Simple Line Interface Method)**
- Interface constructed using straight lines parallel to the coordinate axes
- 6 possible configuration
- Neighboring cells taken into account for flux determination
- Though crude, some reasonable predictions were made

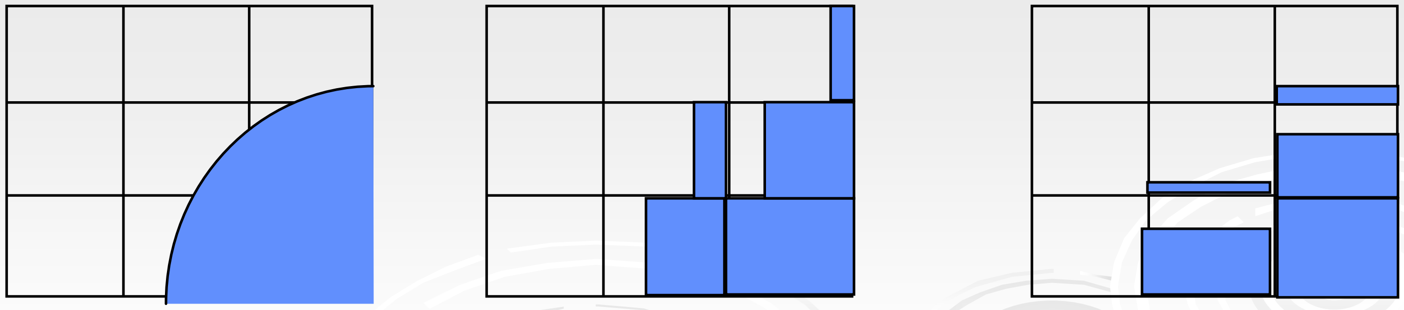

➢ **Hirt and Nichols**

- Interface is horizontal or Vertical (piecewise constant, stair stepped)
- Derivatives of the void field determine whether the interface is horizontal or Vertical
- Derivatives calculated using fractional volumes averaged over several cells

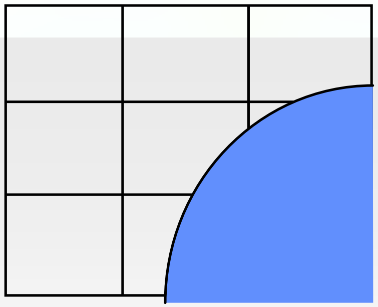

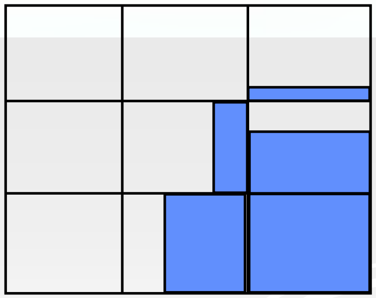

➢ Youngs Method (1982) or PLIC (Piecewise Linear Interface Construction)

- Interfaces - piecewise linear
- Interface has slope and is fitted within a single cell
- Interface slope and fluid position are determined from inspection of 8 neighboring cells

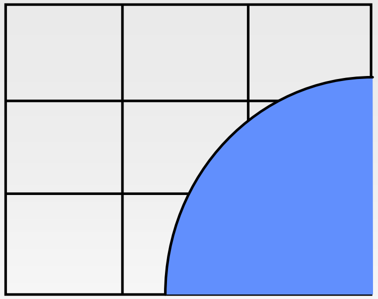

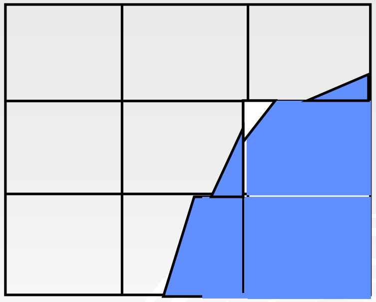

Youngs Method Continued…

- The interface is defined by the interface normal $\hat{n}$ and length l

$$n^x_{i,j} = \frac{1}{8\delta x}(\alpha_{i+1,j+1} + 2\alpha_{i+1,j} + \alpha_{i+1,j-1} - \alpha_{i-1,j+1} - 2\alpha_{i-1,j} - \alpha_{i-1,j-1})$$

$$n^y_{i,j} = \frac{1}{8\delta x}(\alpha_{i+1,j-1} + 2\alpha_{i,j+1} + \alpha_{i-1,j+1} - \alpha_{i+1,j-1} - 2\alpha_{i,j-1} - \alpha_{i-1,j-1})$$

- Position (l) of the interface is so adjusted that it divides the cell into two areas which matches with the volume fraction
- $(\hat{n},l)$ completely locate the interface

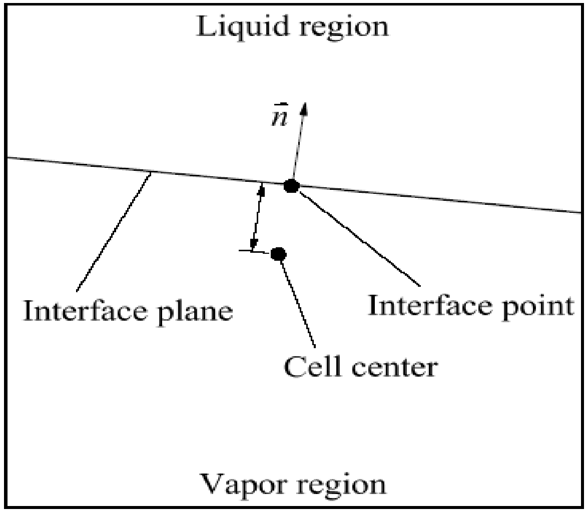

➢ **LVIRA (Least Square Volume of Interface Reconstruction Algorithm,** Puckett et al. (1997))

Properties:

- Piecewise linear approximation in each multifluid cell
- Orientation $\vec{n}$ is optimized by the void fraction of the surrounding cells (3 x 3 block) by minimizing the function

$$G_{ij}(\vec{n},l)=\sum_{\substack{k=-1\\l=-1}}^{1}\left(\alpha_{i+k,j+l}-\tilde{\alpha}_{i+k,j+l}(\vec{n},l)\right)^2$$

where α is the given void fraction and $\tilde{\alpha}$ is the approximation due to the linear interface

- Initial value of $\vec{n}$ is taken from Young's method
- Modify l and $\vec{n}$ till G_{ij} is minimized such that,

$$\tilde{\alpha}(\vec{n},l)\approx\alpha$$

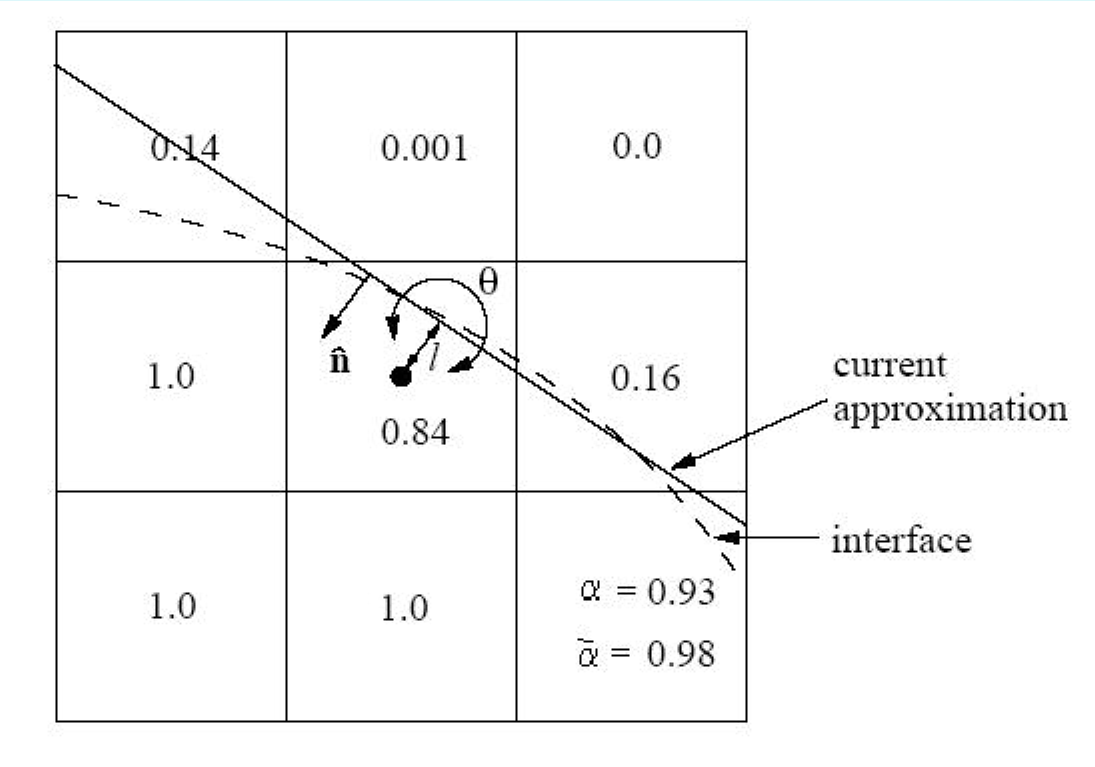

$$G_{ij}(\vec{n},l)=\sum_{\substack{k=-1\\ l=-1}}^{1}\left(\alpha_{i+k,j+l}-\tilde{\alpha}_{i+k,j+l}(\vec{n},l)\right)^{2}$$

- **CLSVOF estimation of normal and curvature (Sussman et al. (2000))**

- Level Set function (*Φ*) is defined as:

$$\phi(\boldsymbol{r},t)\begin{cases} = -d \text{ in gas region} \\ = 0 \text{ at the interface} \\ = +d \text{ in liquid region} \end{cases}$$

where d = d(**r**) is the shortest distance of a point **r** from the interface.

- Normal '**n**' and curvature 'κ' are computed as:

$$\boldsymbol{n} = \frac{\nabla \phi}{|\nabla \phi|} \quad \text{and}$$

$$\kappa = -\nabla \cdot \boldsymbol{n}$$

CST Continued…

Calculation of ρ and μ

$$\rho(\tilde{\alpha}) = \rho_l(\tilde{\alpha}) + \rho_g(1-\tilde{\alpha})$$

$$\mu(\tilde{\alpha}) = \mu_l(\tilde{\alpha}) + \mu_g(1-\tilde{\alpha})$$

One ***full augmented momentum equation*** can be written for all cells: (liquid, gas and two-phase cells)

$$\rho(\tilde{\alpha})\left(\frac{\partial\vec{v}}{\partial t} + \vec{v}.\nabla\vec{v}\right) = -\nabla p + \rho(\tilde{\alpha})\vec{g} + \nabla.\left\{\mu(\tilde{\alpha})\left[\nabla\vec{v} + (\nabla\vec{v})^T\right]\right\} + \sigma k\nabla\tilde{\alpha}$$

- f_{sv} = Volume force due to surface tension = $f_{sa}\delta_s$, δ_s = Dirac delta function

$$\delta_s = \begin{cases} 1 \text{ at two phase cell} \\ 0 \text{ at single phase cell} \end{cases}$$

- f_{sa} = surface tension force pet unit interfacial area = normal force + tangential force = $\sigma\kappa\hat{n} + \nabla_s\sigma$
- Neglecting temperature or concentration change, surface tension constant so $\nabla_s\sigma$ can be neglected.

Modified momentum equation:

Using the concept of diffusing the interface over a thin region according to Brackbill et al. [1992], J. Comput. Phys.

$$\rho(\tilde{\alpha})\left(\frac{\partial\vec{V}}{\partial t} + \nabla\cdot\left(\vec{V}\vec{V}\right)\right) = -\nabla P + \rho(\tilde{\alpha})\vec{g} + \nabla\cdot\left[\mu(\tilde{\alpha})\left(\nabla\vec{V} + \left(\nabla\vec{V}\right)^T\right)\right] + \sigma\kappa\nabla\tilde{\alpha}$$

CST Continued…

- **Heaviside function**: An alternative to Kernal K_8 smoothening in CLSVOF.

- $$H(\phi)=\begin{cases} 0 \ if \ \phi<-\in \\ \frac{1}{2}+\frac{\phi}{2\in}+\frac{1}{2\pi}\left\{\sin\left(\frac{\pi\phi}{\in}\right)\right\} \ if -\in\leq\phi\leq\in \\ 1 \ if \ \phi>\in \end{cases}$$

- Smoothened density and viscosity field:

$$\rho(\phi)=\rho_g\left(1-H(\phi)\right)+\rho_l H(\phi)$$
$$\mu(\phi)=\mu_g\left(1-H(\phi)\right)+\mu_l H(\phi)$$

Solution Technique

- Staggered grid arrangement
- Uniform grid spacing
- FINITE DIFFERENCE discretization scheme
- Convective terms in momentum equation are discretized by ENO SCHEME. All other space derivatives are CENTRAL SCHEME.
- Pressure equation is solved by an iterative method based on preconditioned conjugate gradient BI-CGSTAB scheme.
- The numerical scheme is based on EXPLIXIT TIME ADVANCEMENT.
- Based on the velocity field at the new time step, a COULPED SECOND ORDER OPERATOR SPLIT ADVECTION SCHEME for discretization of the advection of void fraction (F) and level-set function (ϕ).
- The solution scheme is SECOND ORDER IN SPACE and FIRST ORDER IN TIME.

Secondary drops without splashing (animation)

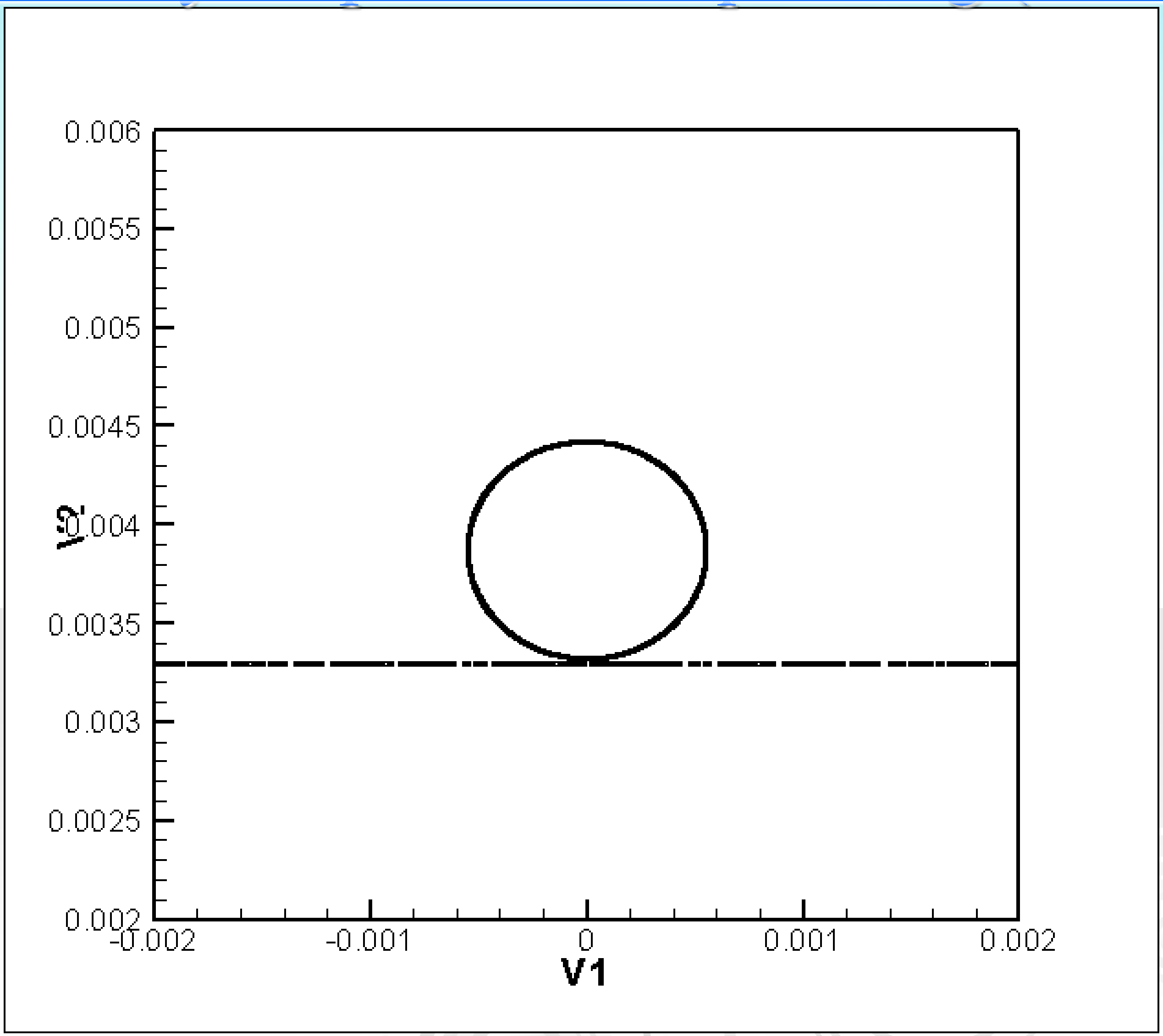

Coalescence cascade

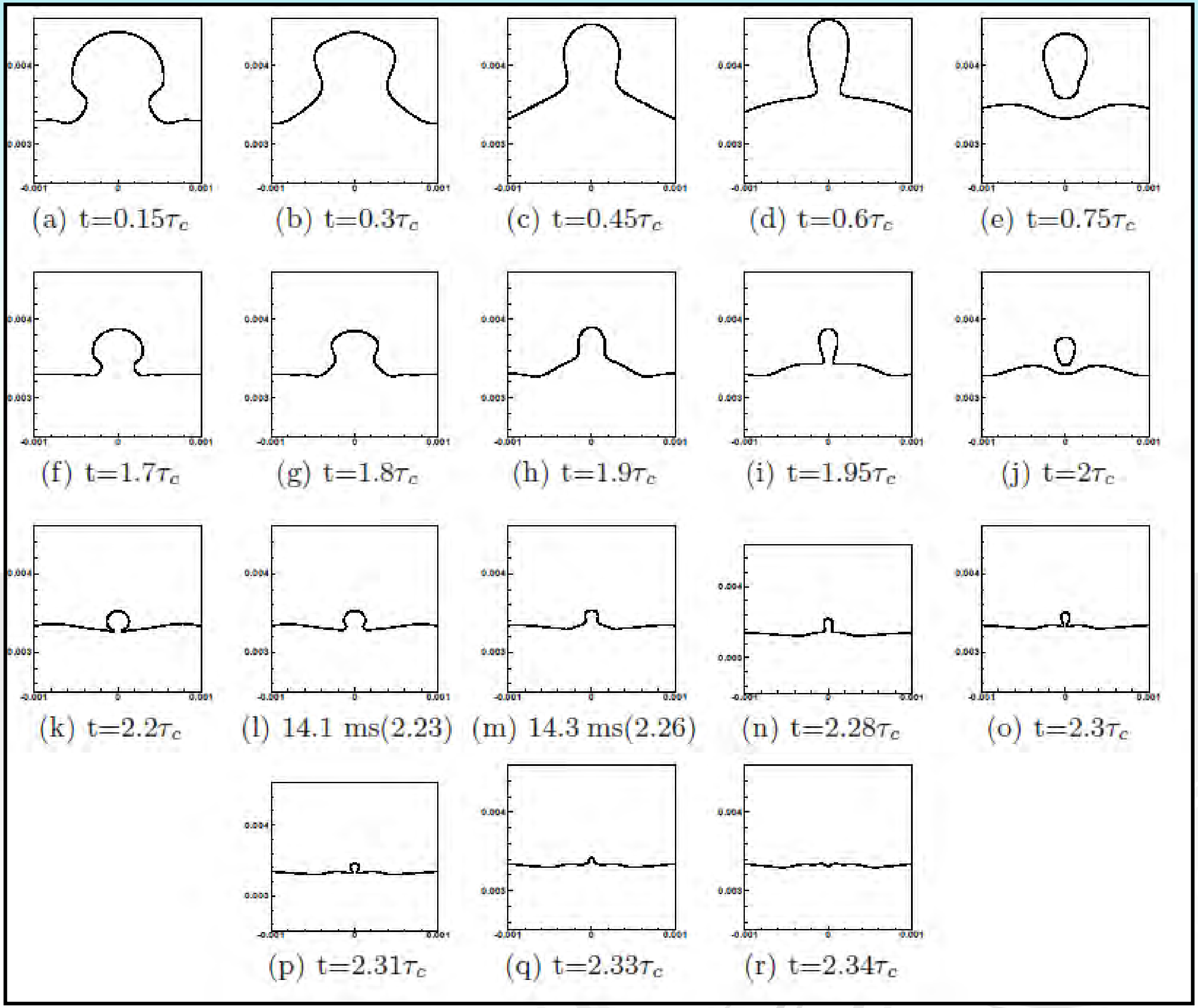

$Oh_1 = 0.0058$,

$Oh_2 = 0.0177$,

$Bo = 0.0958$

$A = 0.136$

Large drops cause complete coalescence

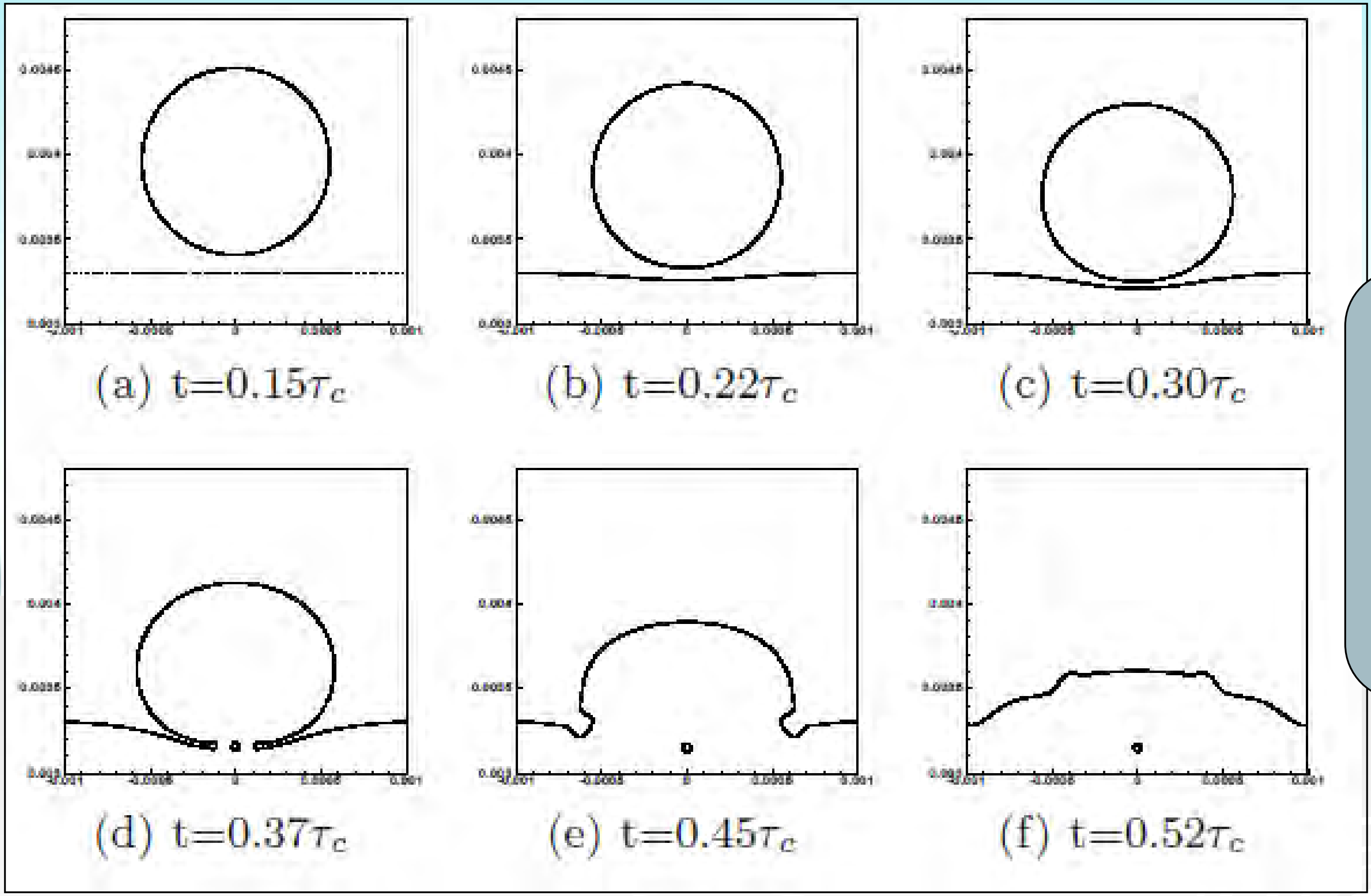

$Oh_1 = 0.0057,$

$Oh_2 = 0.114,$

$Bo = 9.83$

$A = 0.149$

Different regimes

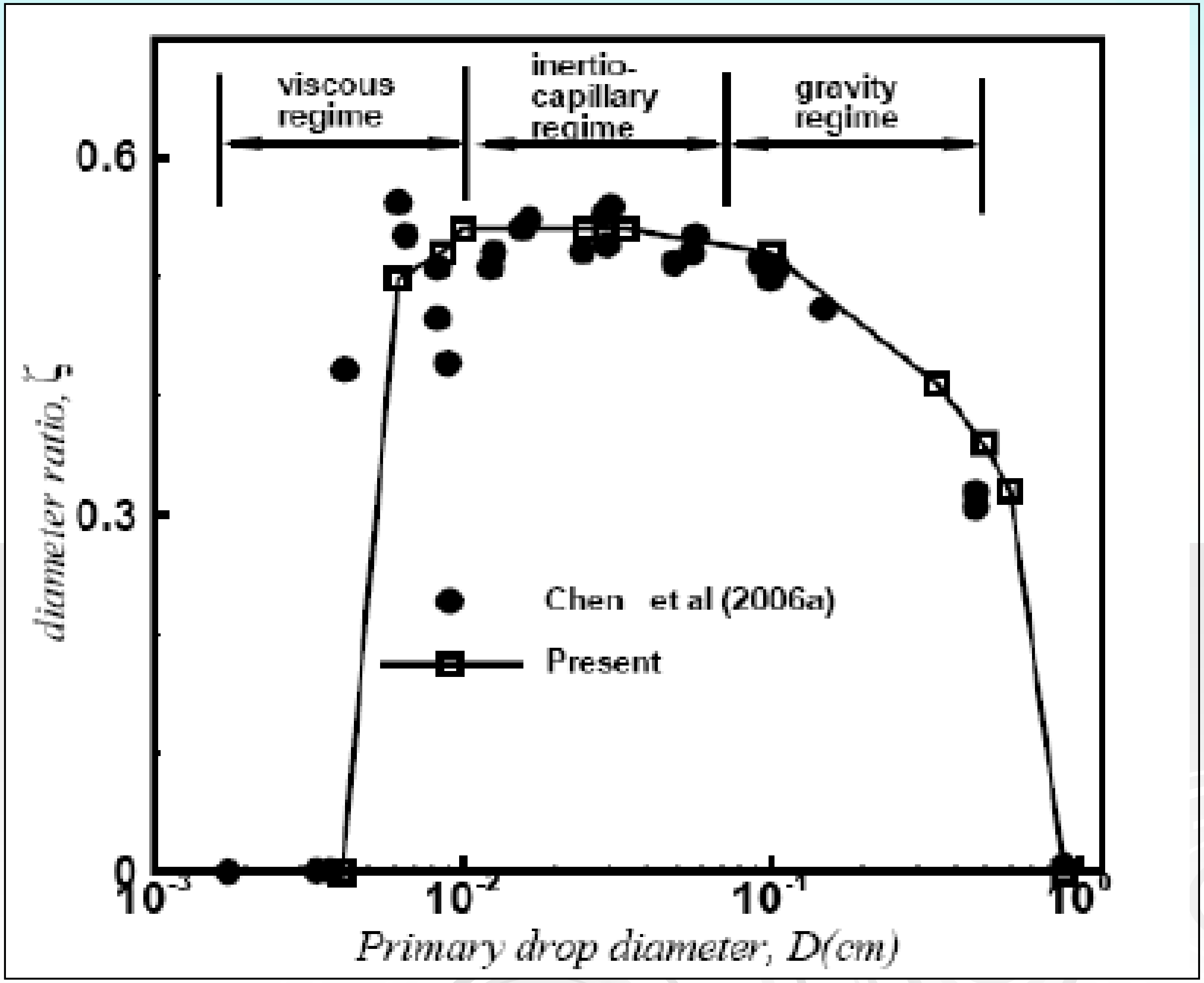

- Charles & Mason (1960) have suggested that the partial coalescence was due to a Rayleigh-Plateau instability.

- Blanchette & Bigioni (2006) have argued that it is the convergence of the capillary waves on the drop apex which leads to secondary drop pinch off.

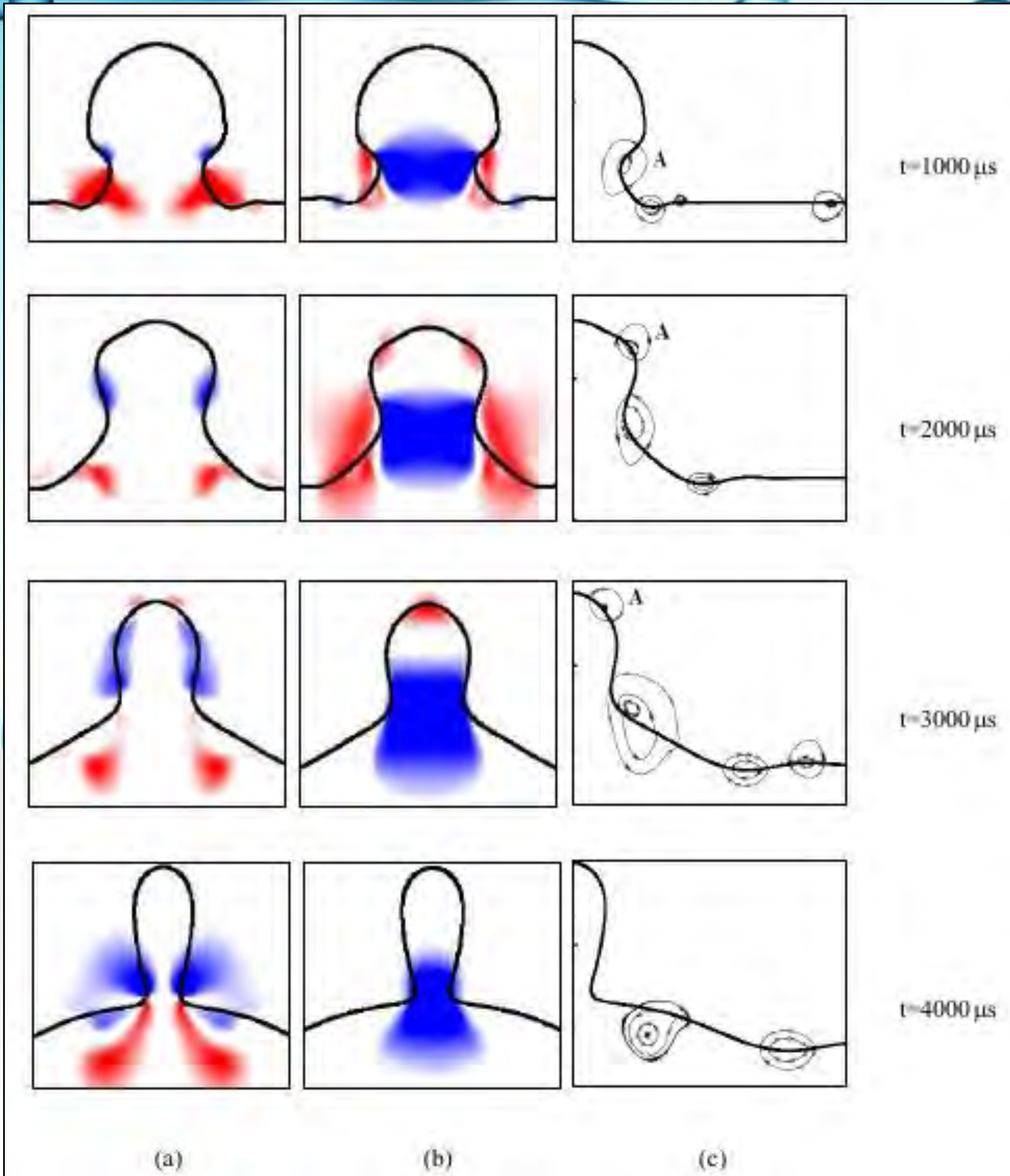

(a) Horizontal velocity contour

(b) Vertical velocity contour

(c) Streamline

Red: positive value
Blue: negative value

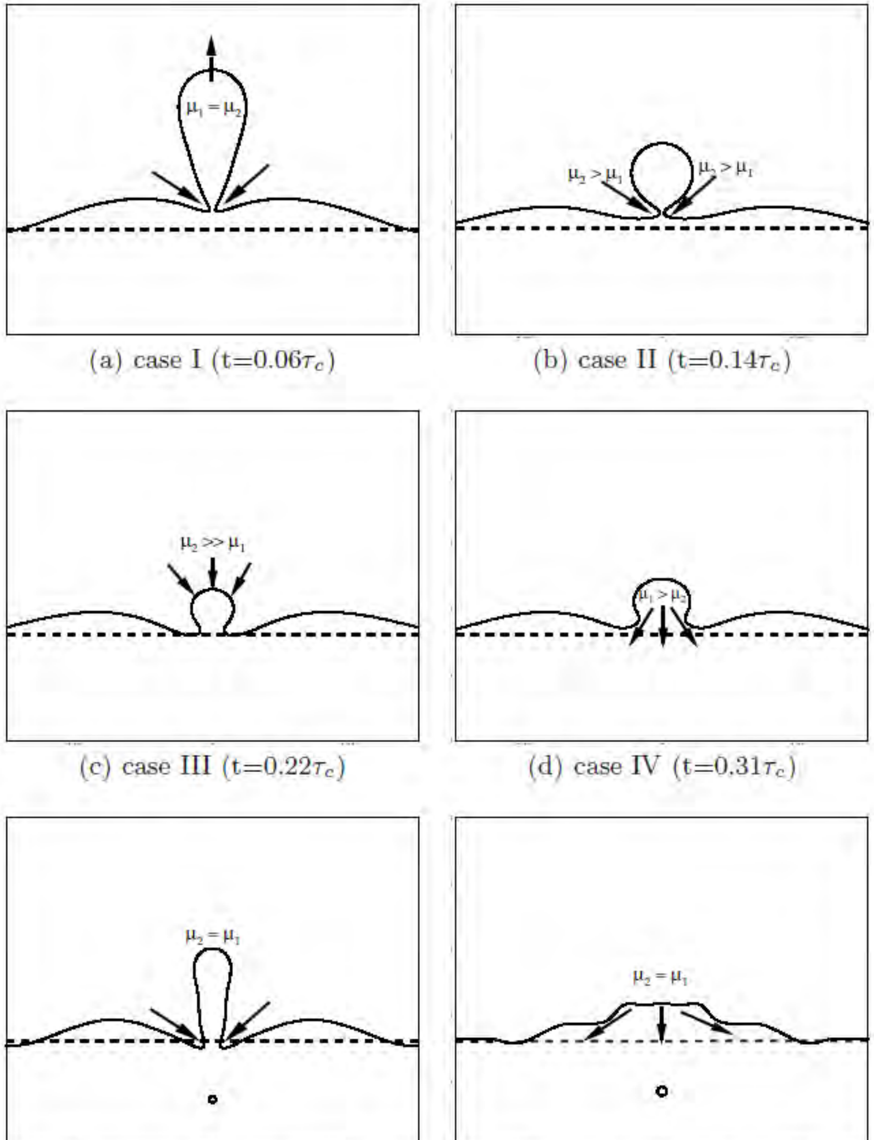

(a) case I (t=0.06τ_c)
(b) case II (t=0.14τ_c)
(c) case III (t=0.22τ_c)
(d) case IV (t=0.31τ_c)
(e) case V (t=0.39τ_c)
(f) case VI (t=0.47τ_c)

Case I : $Oh_1 \approx Oh_2$, Bo is medium

Case II : $Oh_1 < Oh_2$, Bo is medium

Case III : $Oh_1 << Oh_2$, Bo is medium

Case IV : $Oh_1 > Oh_2$, Bo is medium

Case V : $Oh_1 \approx Oh_2$, Bo > medium

Case VI : $Oh_1 \approx Oh_2$, Bo >> medium

- From our study the important criterion for partial coalescence is the increasing horizontal momentum of the drop relative to the vertical momentum. This can be accomplished either by changing the viscosity or by changing the gravity within limits.

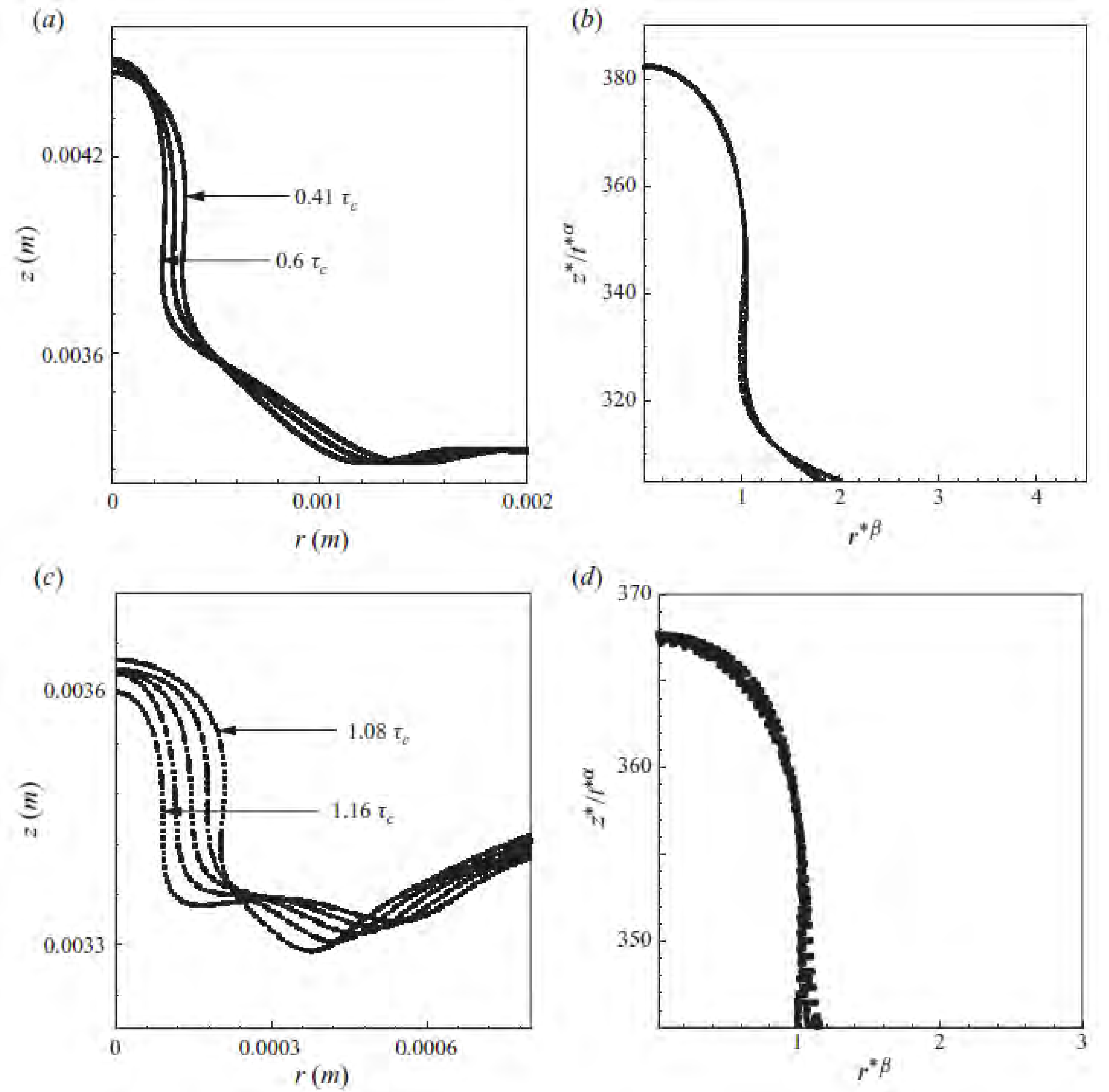

Self-similarity during column formation at TRANSITION ZONE

Acknowledge: Professor Stephane Zaleski of UPMC, Paris

A new bubble entrapment zone

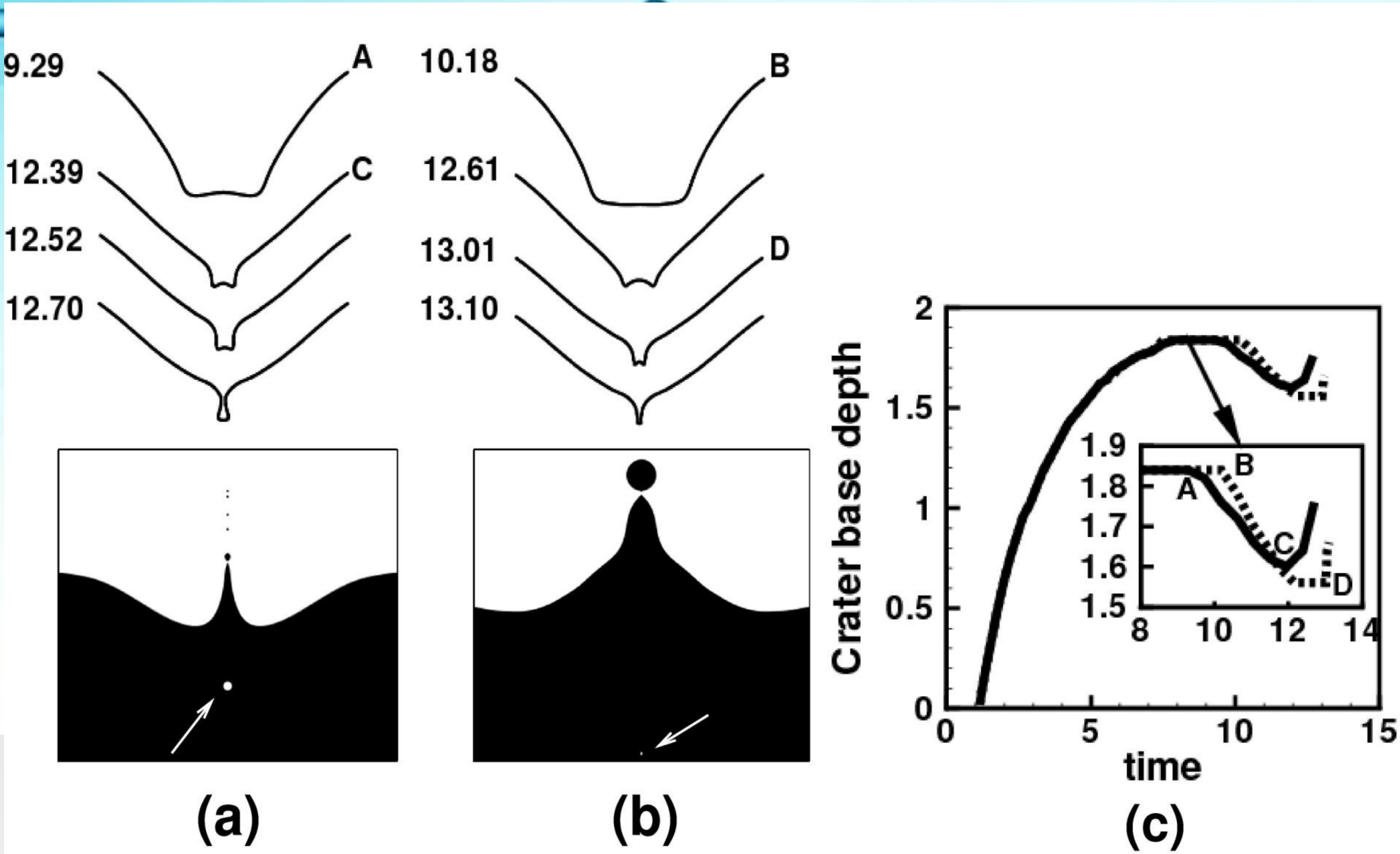

Different crater and jet shapes during large bubble entrapment (Fr =100,We =150) and small bubble entrapment (Fr=100,We= 160) phenomena.

Acknowledge: D. Morton, J. L. Liow and D. E. Cole of UNSW, Australia

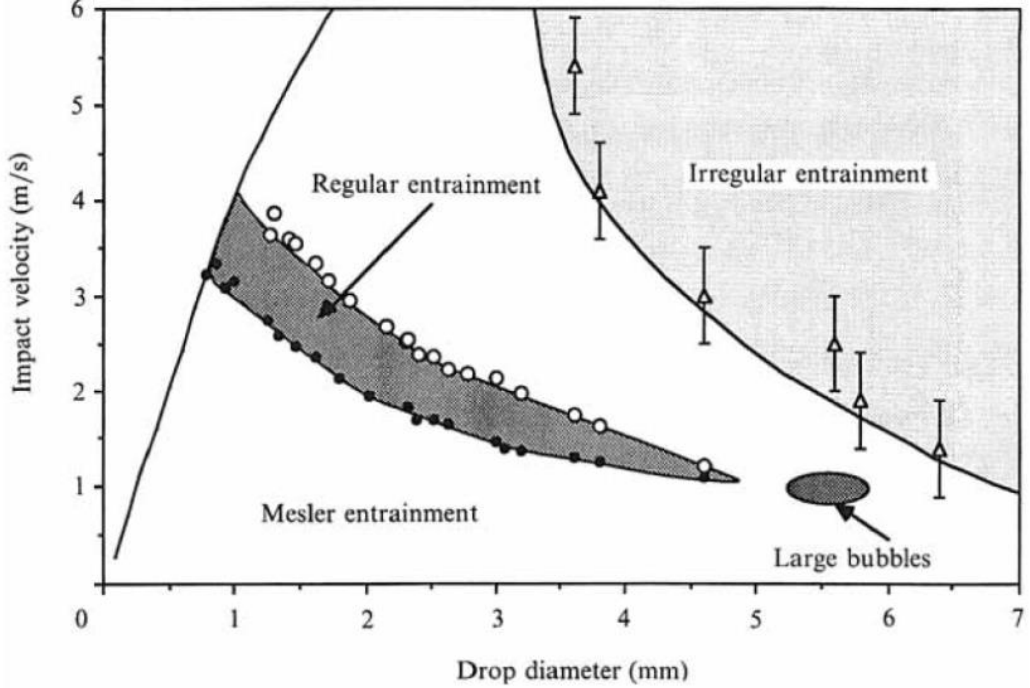

Pumphrey & Crum J. Fluid Mech, 1990

$$Lower: We = 41.3 Fr^{0.179}$$

$$Upper: We = 48.3 Fr^{0.247}$$

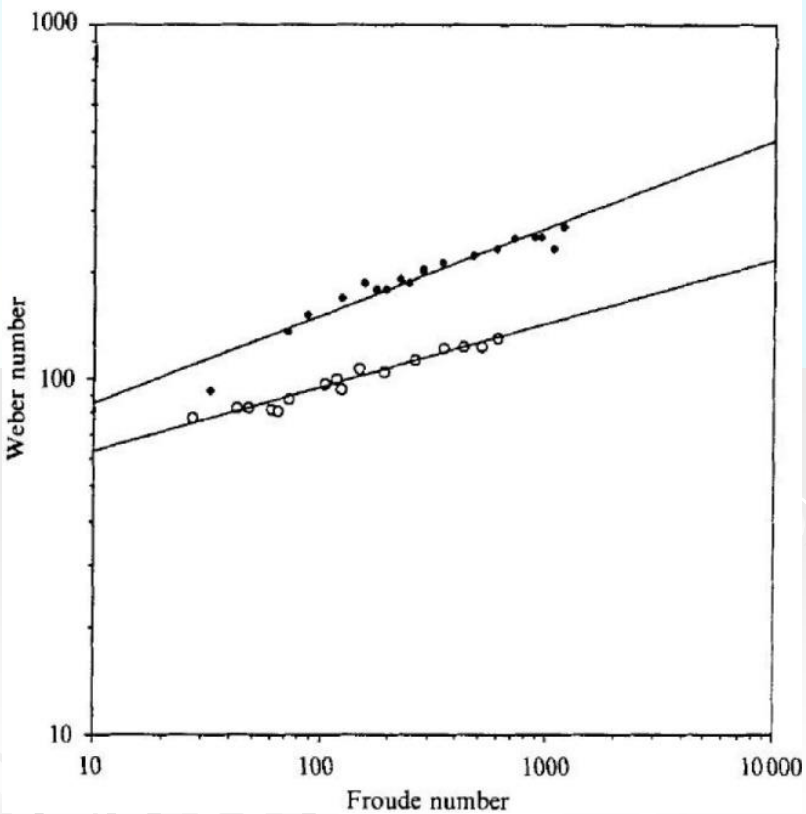

Oguz & Prosperetti J. Fluid Mech, 1990

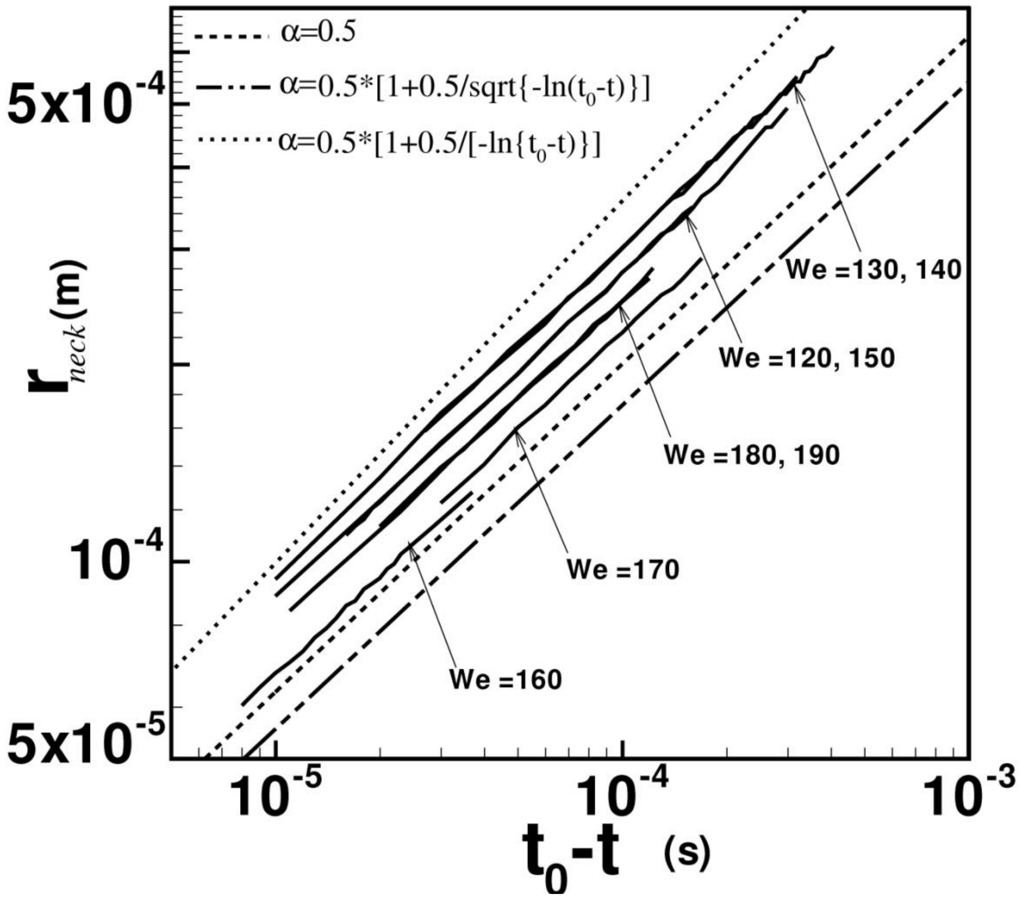

Rayleigh Plesset equation (low viscosity)

$$\ddot{r} + \dot{r}^2 = 0 \Rightarrow r_{min} = A(t_0 - t)^{1/2},$$

$$A = (\sigma R / \rho)^{1/4} = 0.02$$

Keim *et al.*(2006) $\alpha = 0.56 \pm 0.03$

Thoroddsen *et al.*(2007) $\alpha = 0.57 \pm 0.03$

Gordillo *et al.*(2006)

$$\alpha = 0.5 \times \left[1 + 0.5 / \left[-\ln(t_0 - t)\right]\right]$$

Eggers *et al.* (2007)

$$\alpha = 0.5 \times \left[1 + 0.5 / \sqrt{-\ln(t_0 - t)}\right]$$

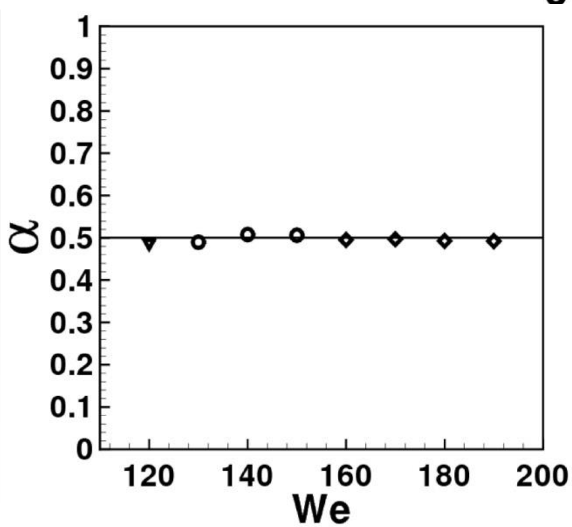

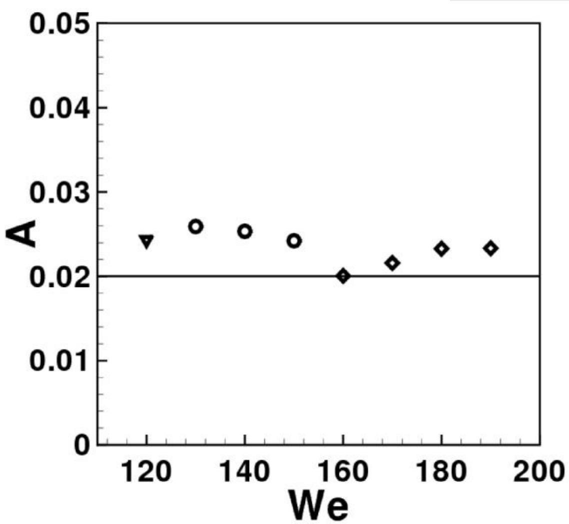

$$\alpha = 0.5 \pm 0.02, A = 0.02 \pm 0.006$$

BUBBLE ENTRAPMENT

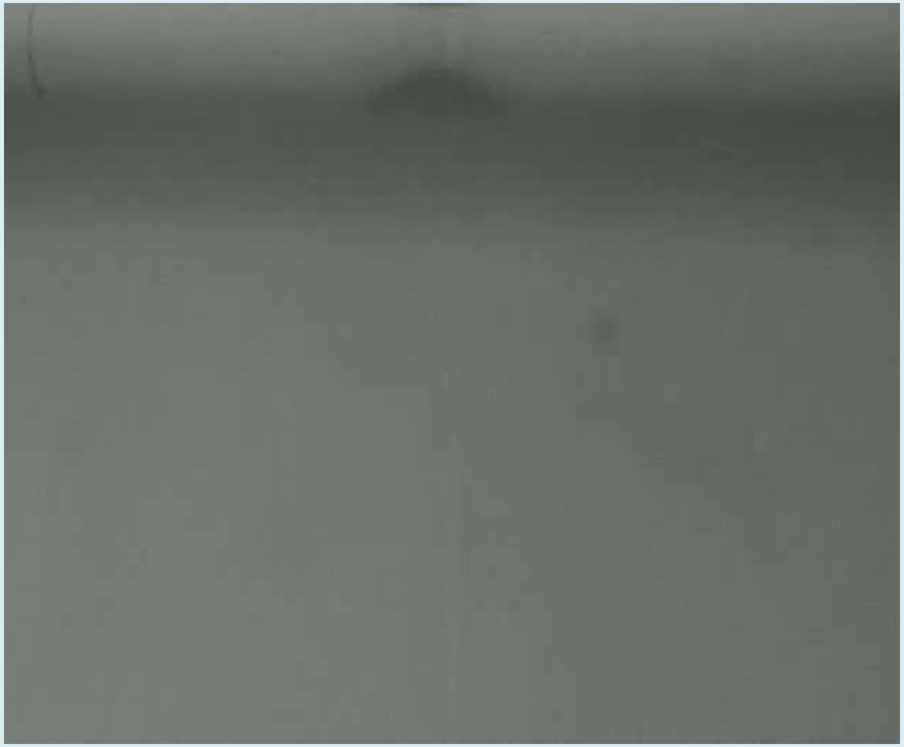

Experiment

Formation of Jet and Bubble Entrapment

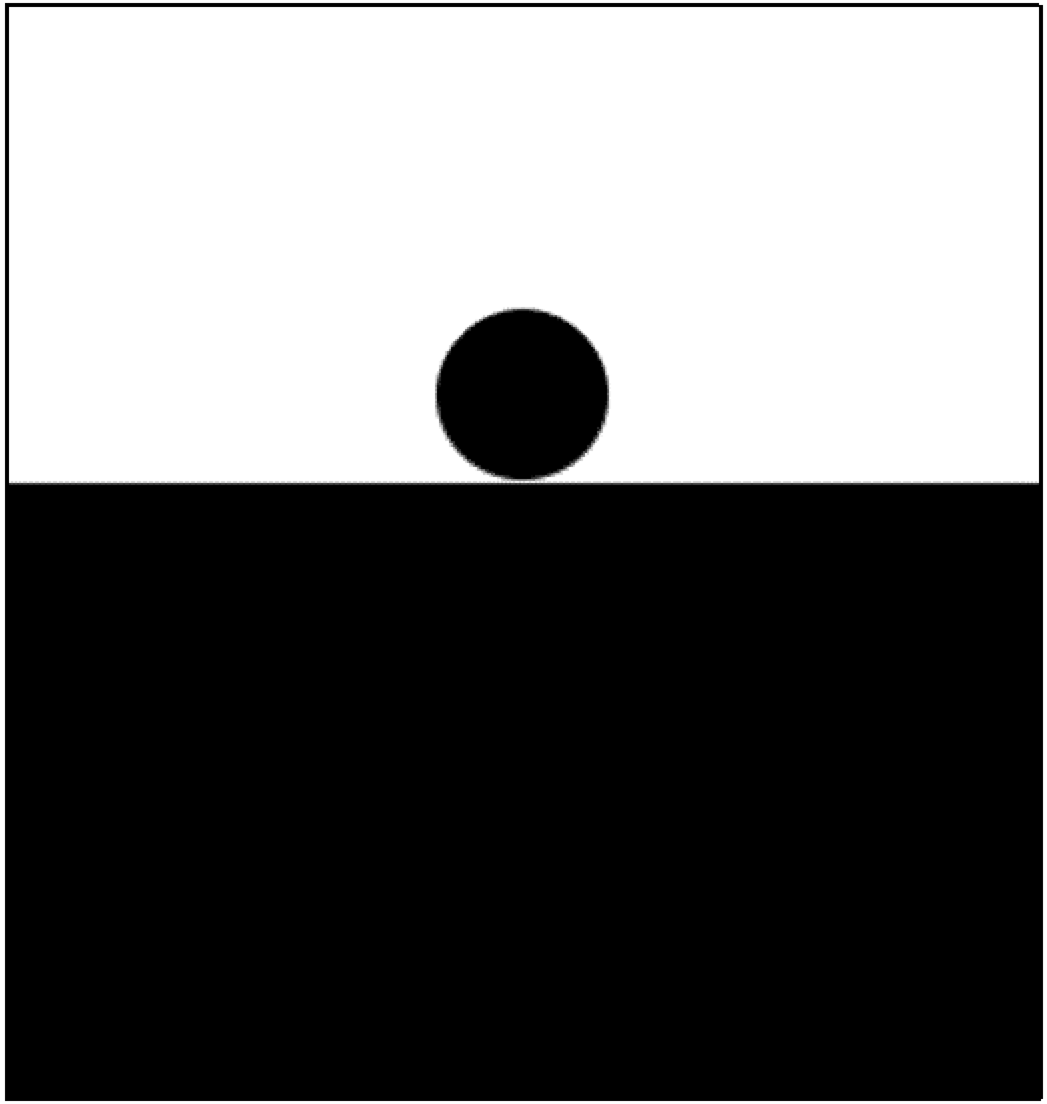

Large Bubble Entrapment

Let us revisit..

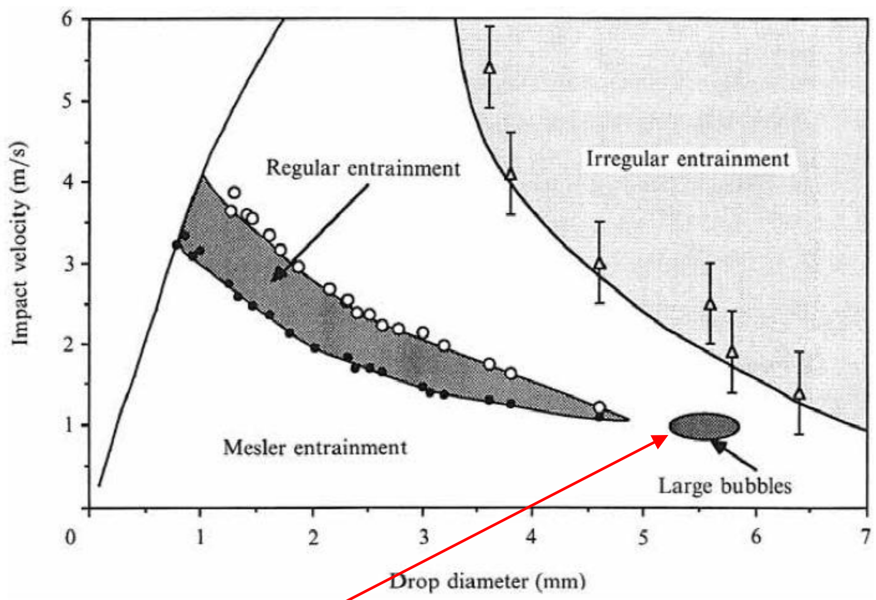

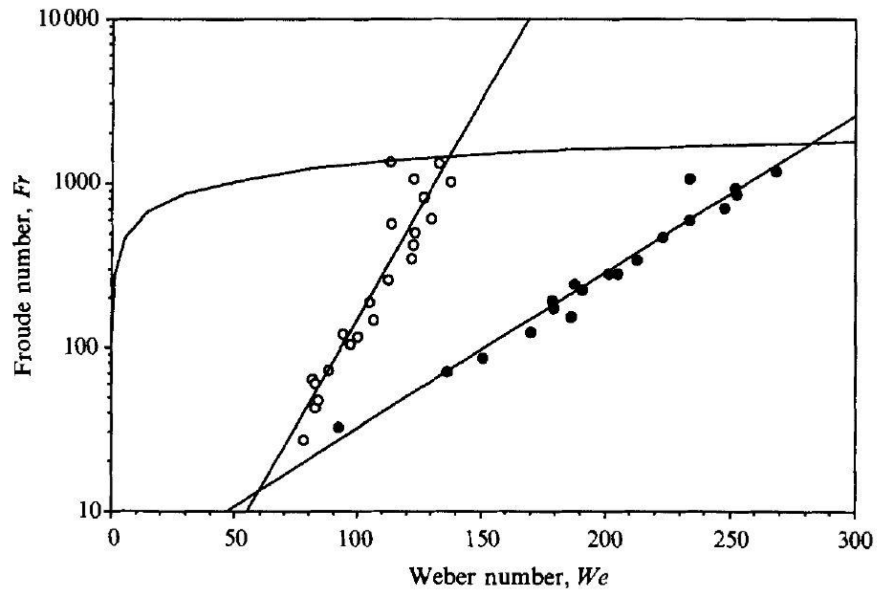

- Small large bubble entrapment regime

❖ Classification map proposed by Pumphrey and Elmore (1990)

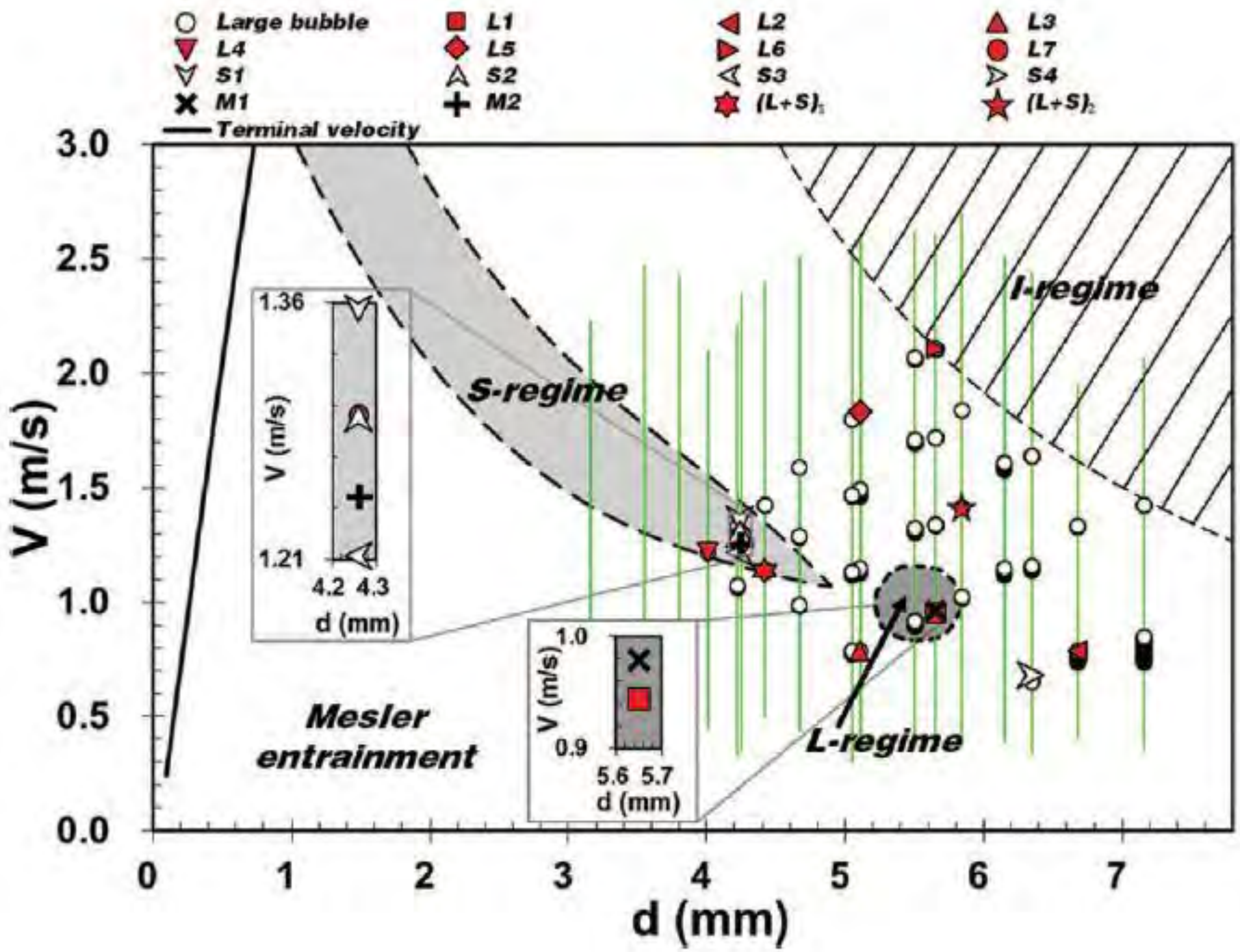

❖ Wang et al.(2013) 'Do we understand the bubble formation by a single drop impacting upon liquid surface? ', Phy. Fluid , vol. 25, pp. 101702

An animation of the large bubble entrapment process.

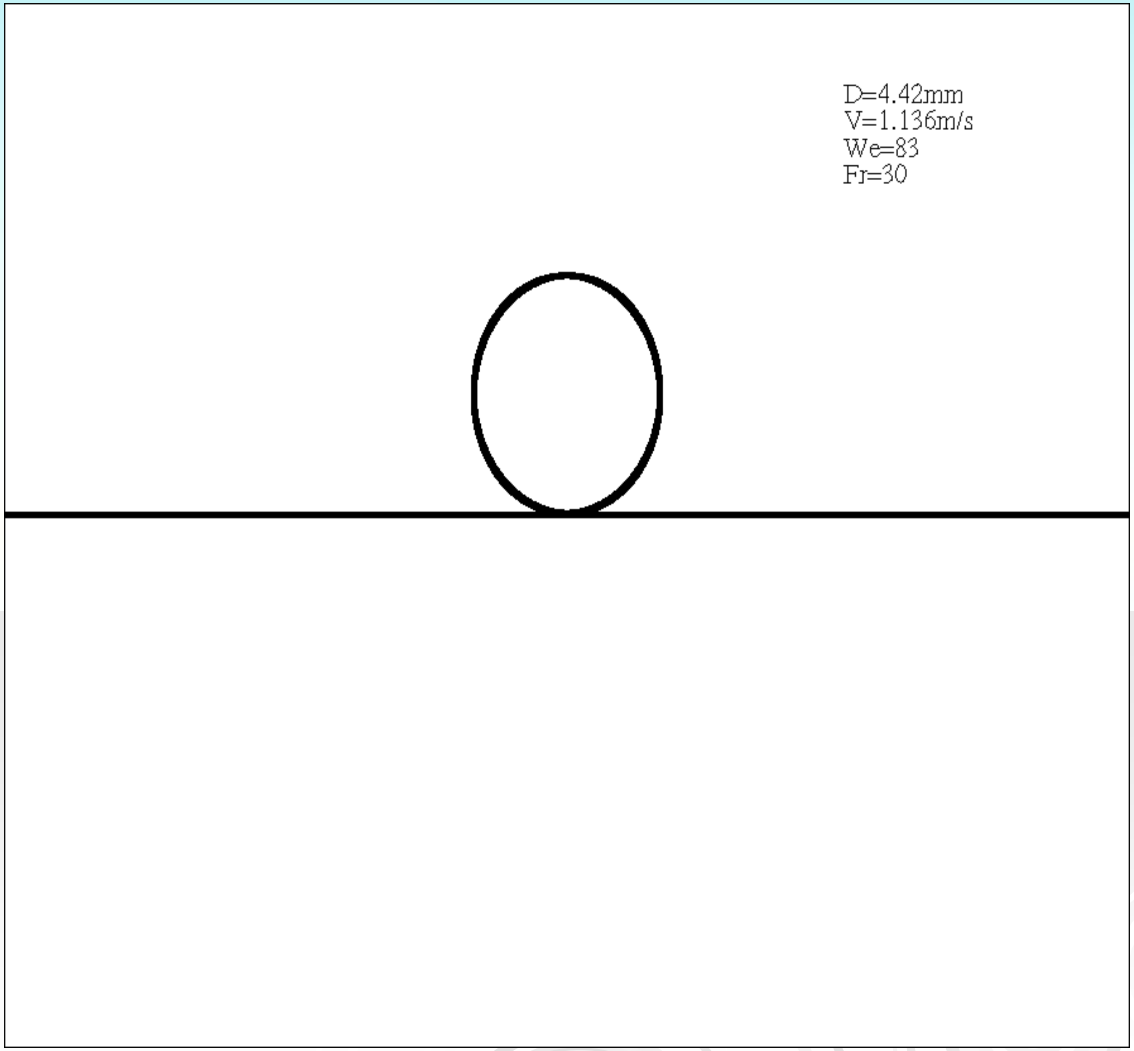

Comparison with experiments

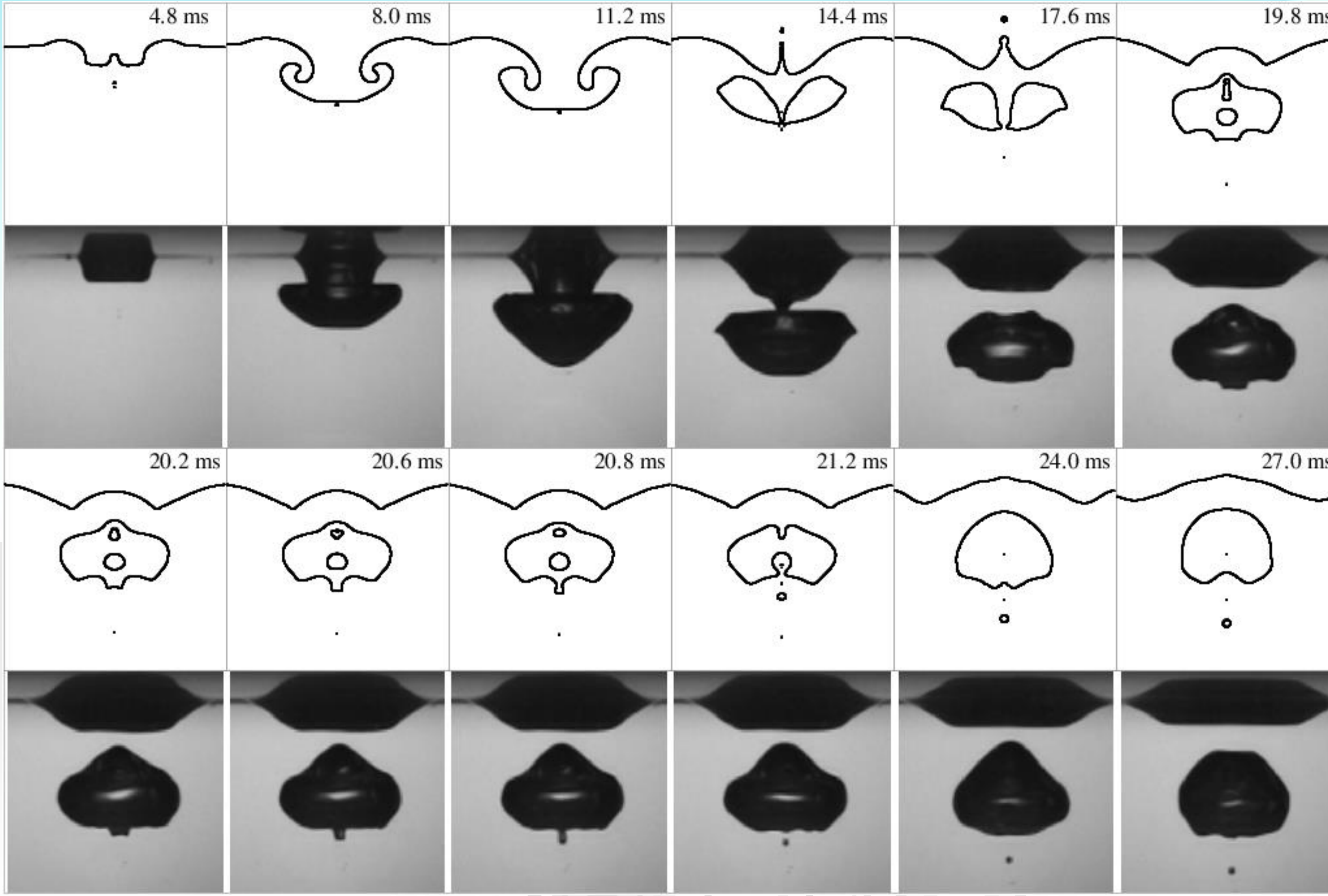

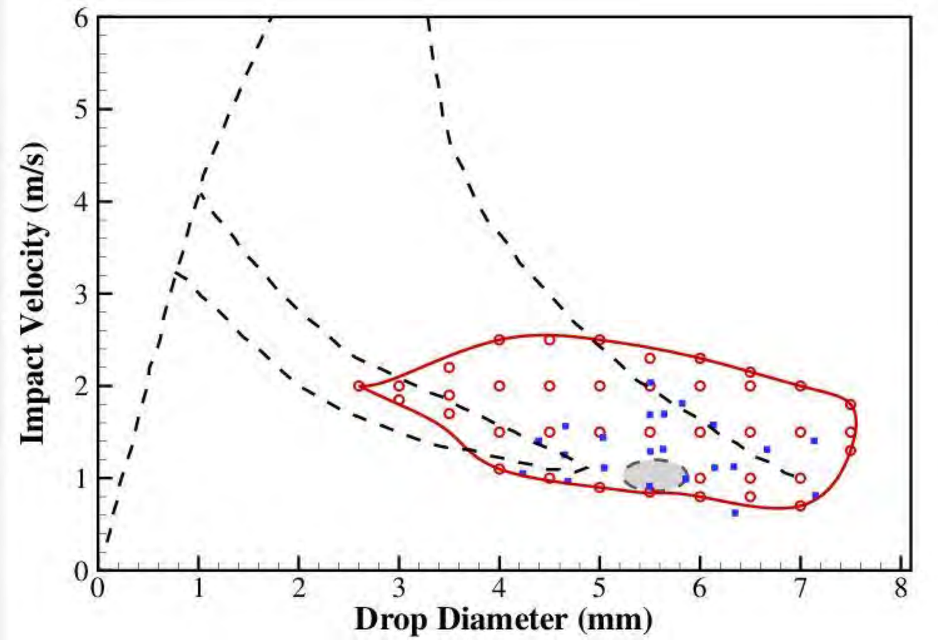

Our Observations

V-D map

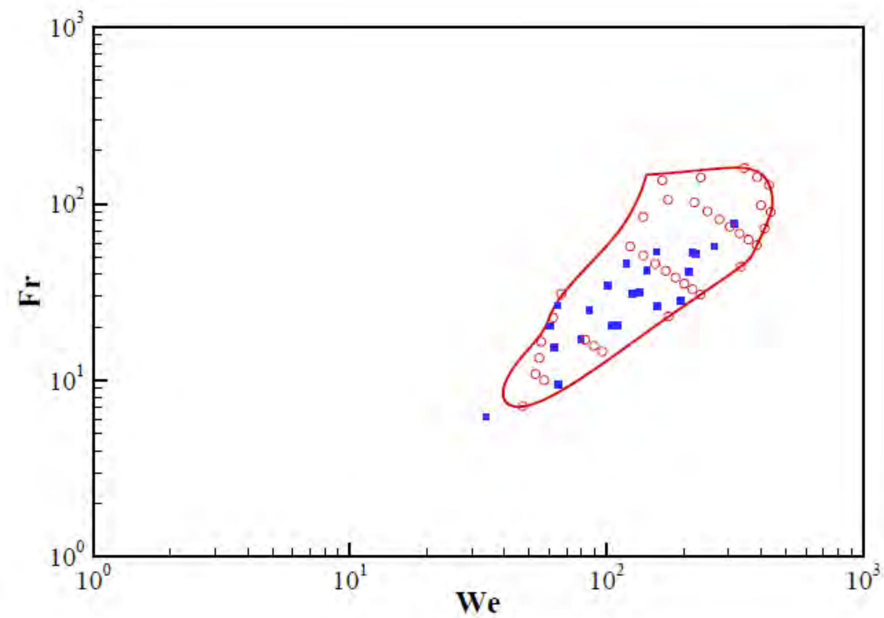

We-Fr map

❖ H. Deka, B. Ray, G. Biswas, A. Dalal, P. Tsai and A. B. Wang, The regime of large bubble entrapment during a single drop impact on a liquid pool. Physics of Fluids 29 (9),092101 (2017).

Vortex Ring

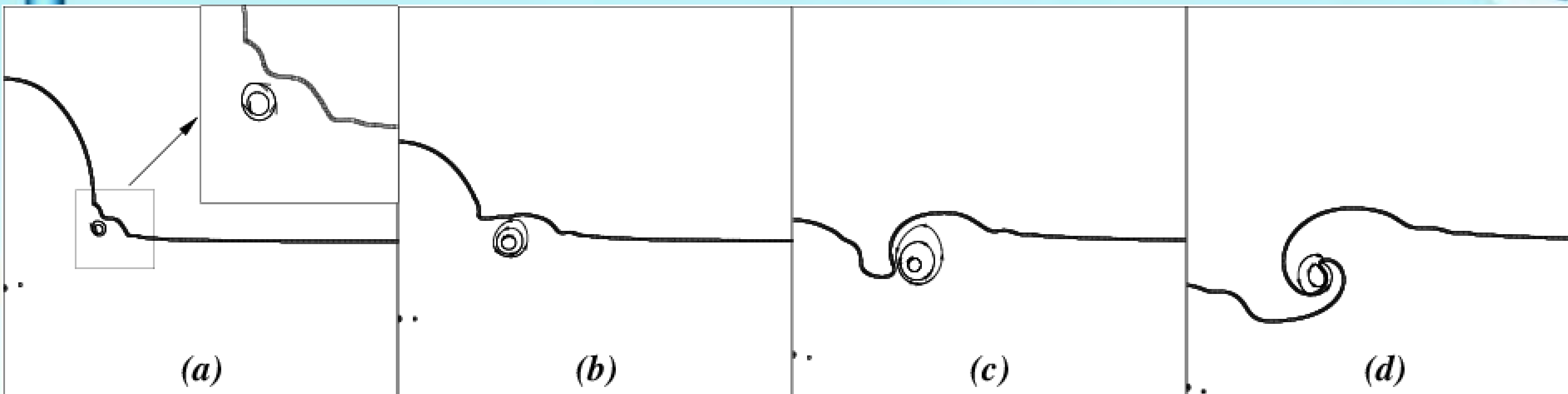

- Vortex ring originate at the corner and penetrate into the pool.
- Vortex ring curls-up the liquid near the interface and forms the roll jet.

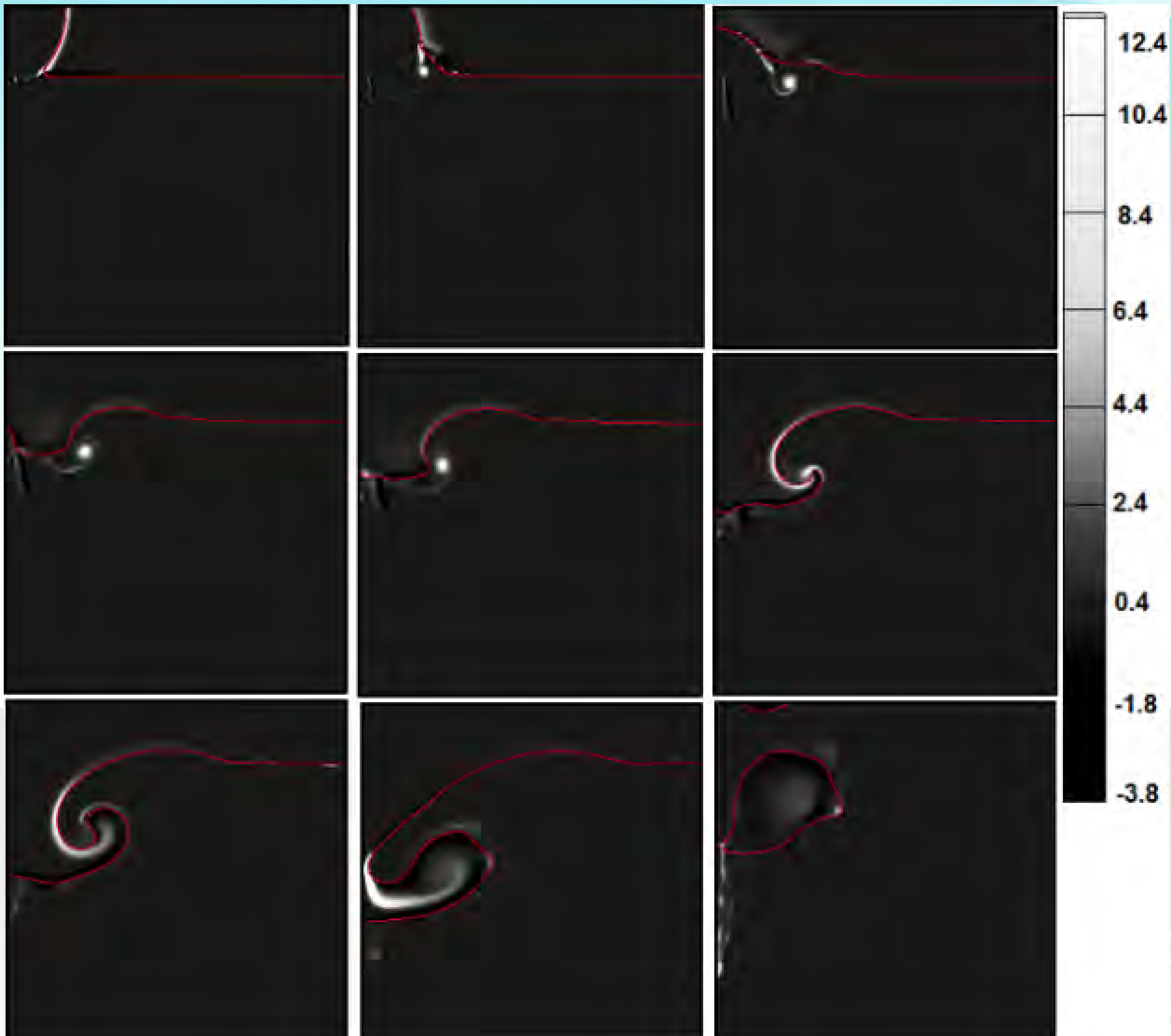

Vorticity plot

V = 2.8 m/s, We = 325, Fr = 266

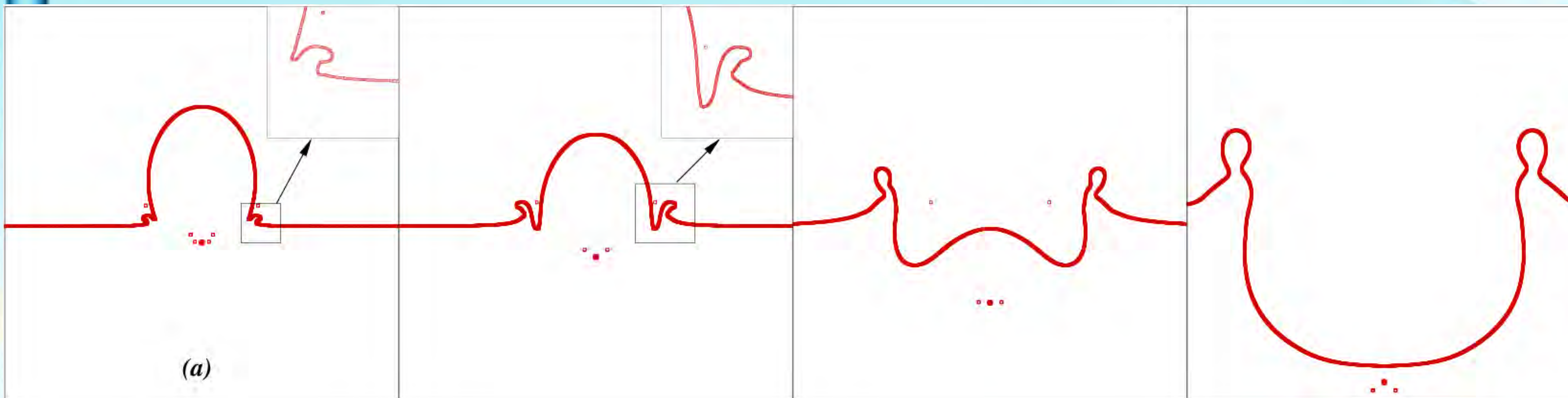

V = 2.0 m/s, We = 165, Fr = 140

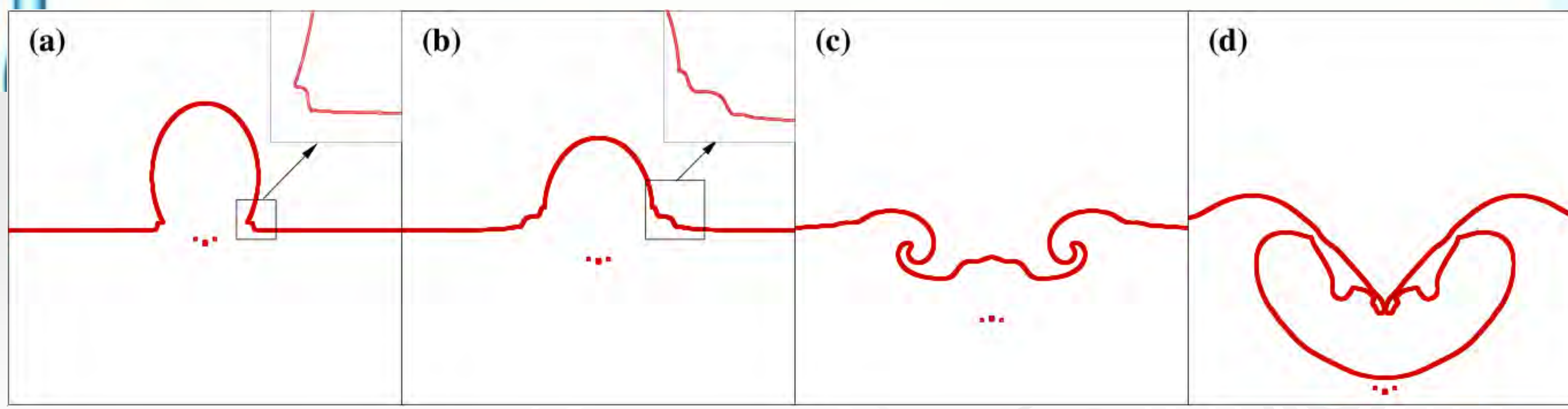

- Formation of merged ejecta-lamella sheet prevents the vortex ring penetration.

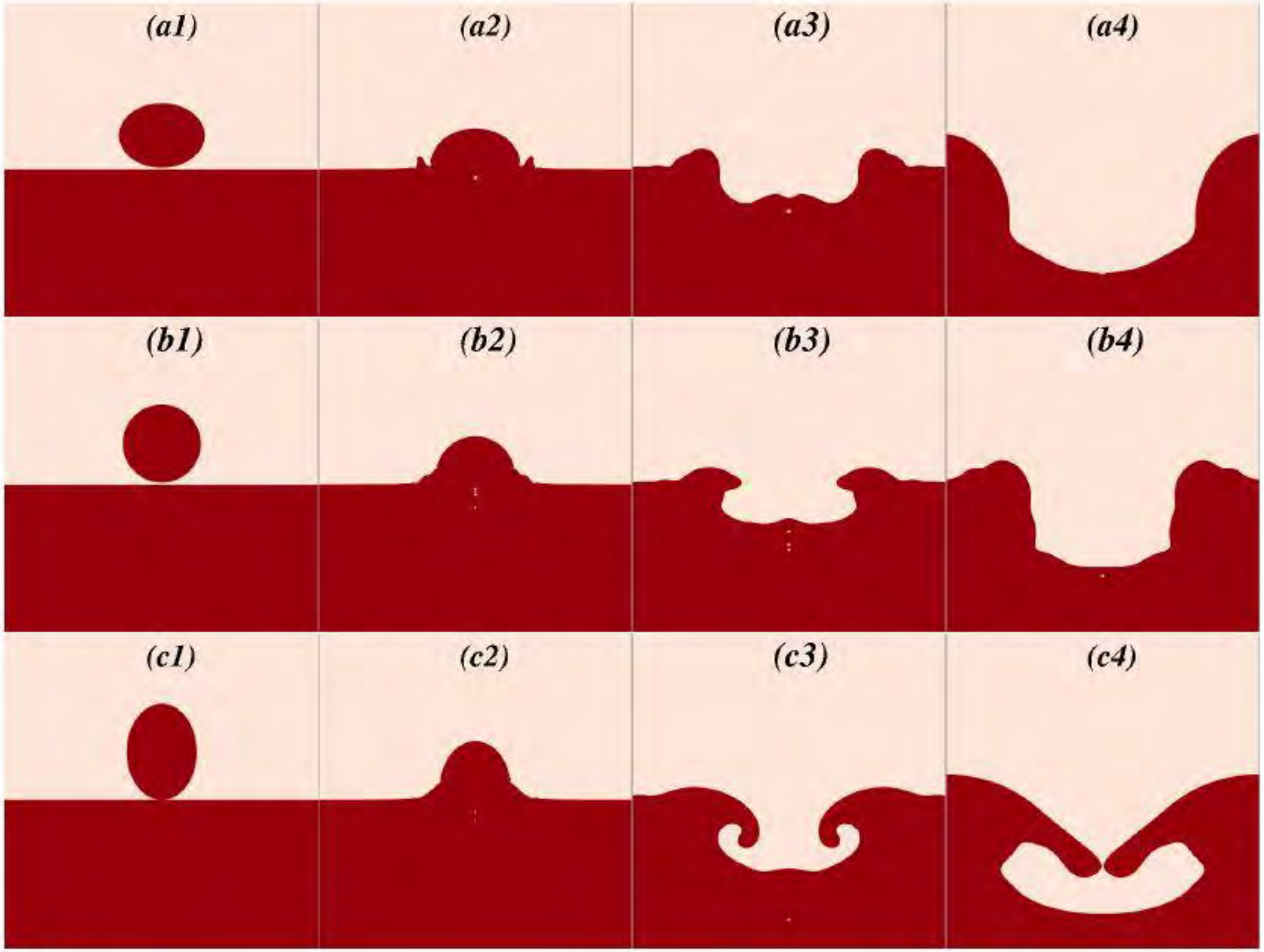

$AR = 0.7$

$AR = 1.0$

$AR = 1.37$

Comparison for different shapes

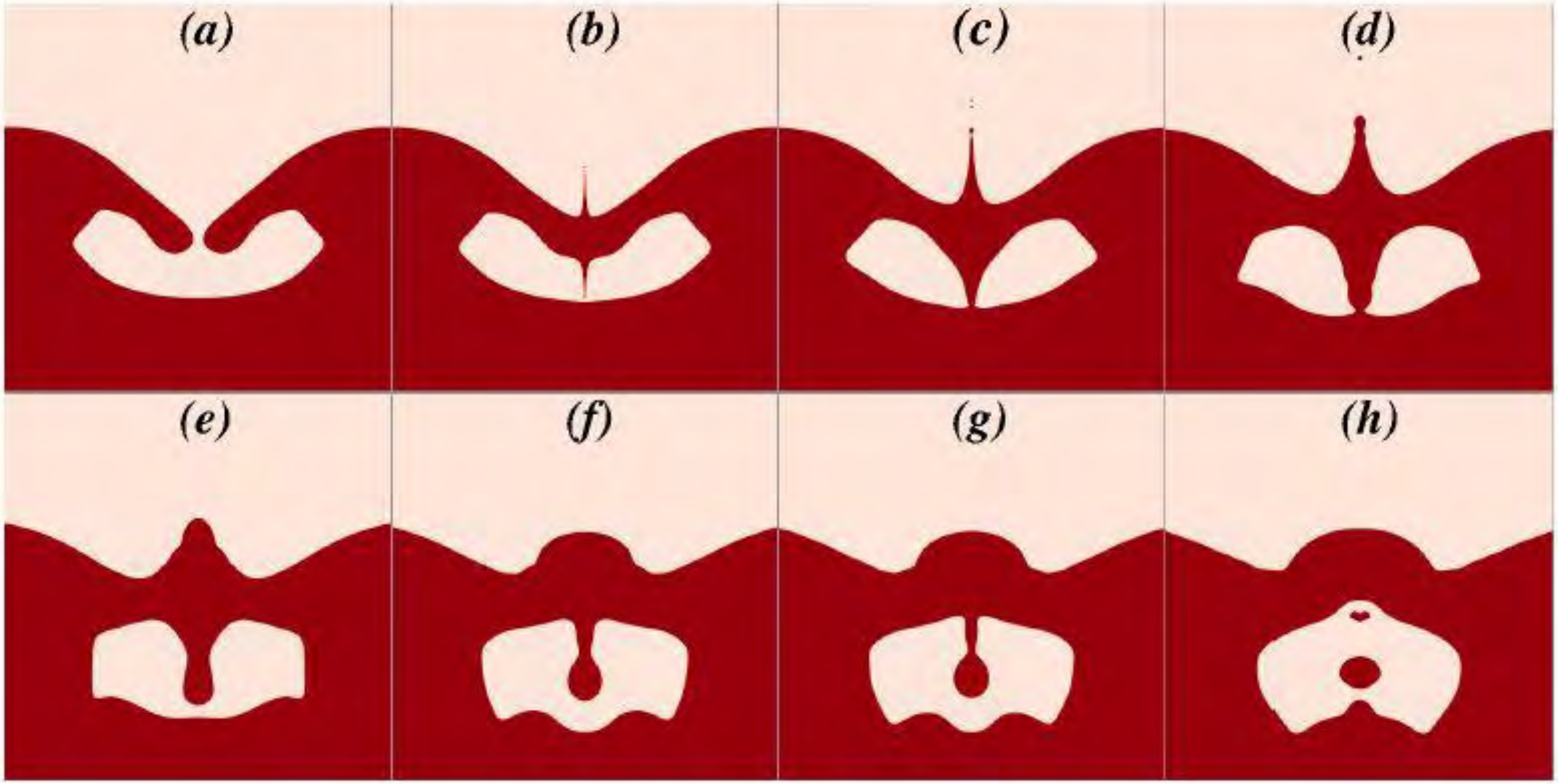

Jet formation

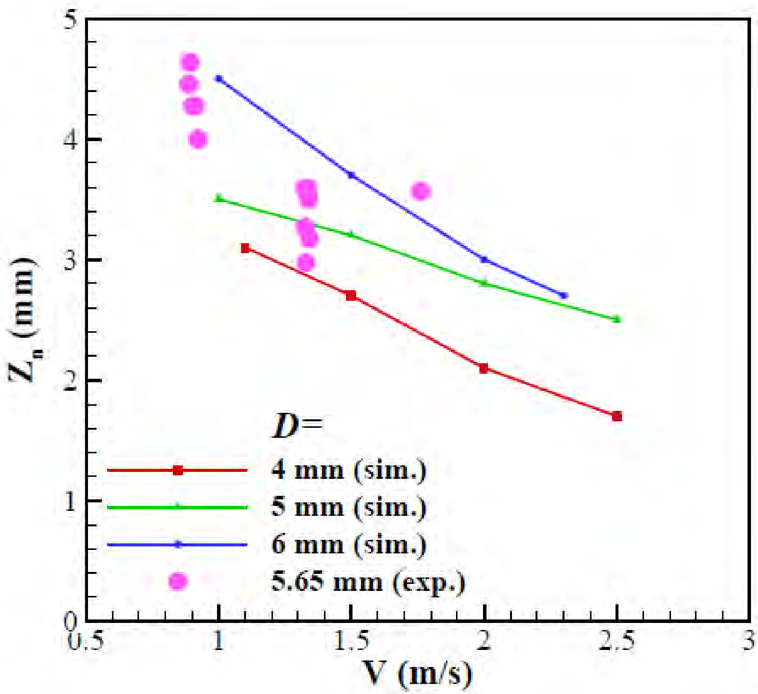

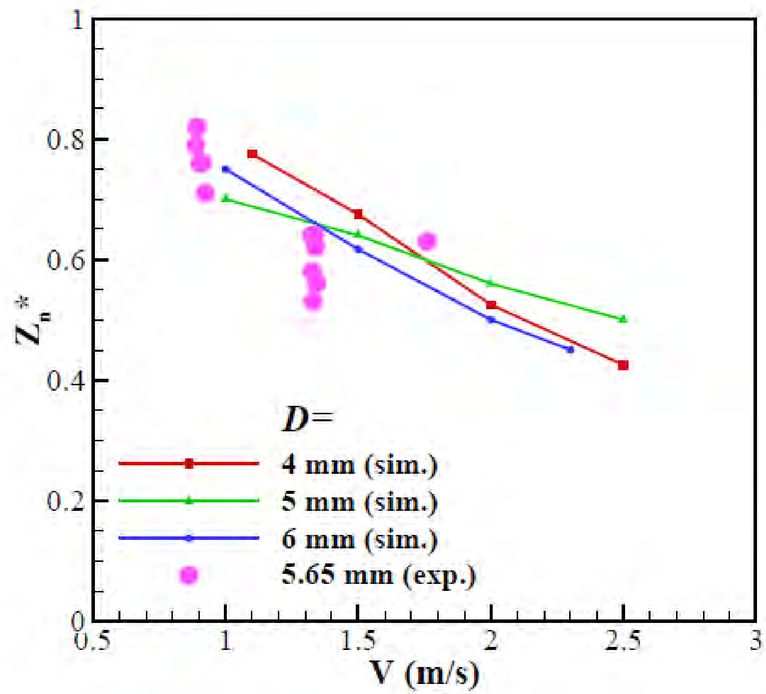

- Enclosure depth decreases with increase in impact velocity
- Little discrepancy between experimental and numerical results arose because of changed aspect ratio.

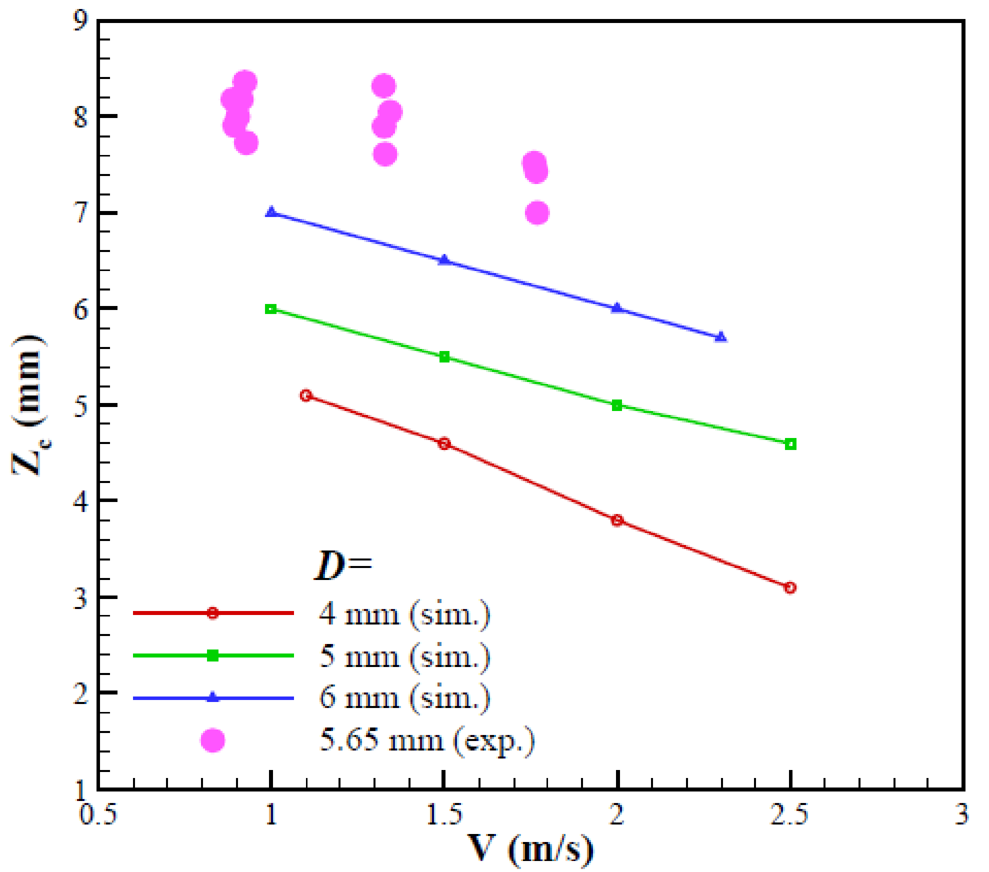

- Crater depth decreases with increase in impact velocity
- Higher impact velocity produces stronger vertical flow near the interface.
- Vortex starts early interaction with the interface.

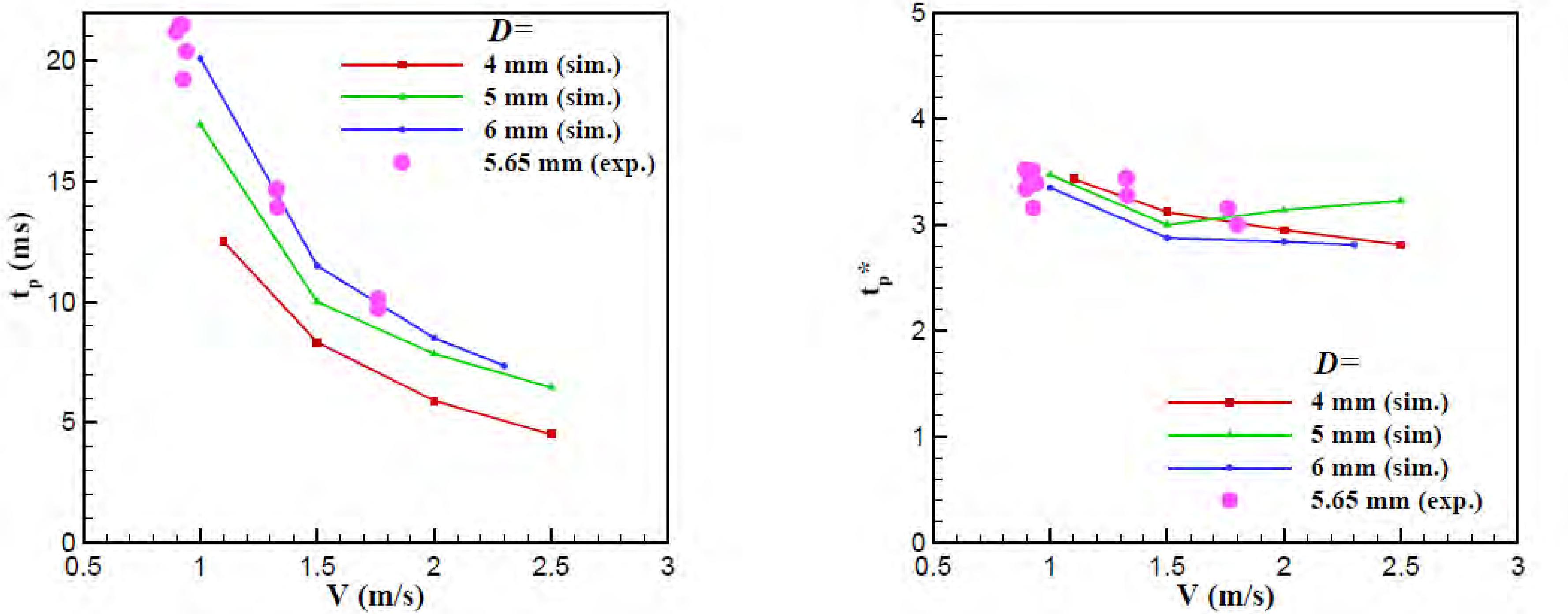

- Higher impact velocity produces stronger vertical flow near the interface.
- Vortex starts early interaction with the interface leading to early pinch-off.
- In non-dimensional time scale, $t_p^* = t_p V / D$ the pinch-off time is nearly constant in all the cases .

Conclusions

- When liquid drop impacts on a **liquid/ liquid or Liquid/ gas interface**, for very small drops and for very large drops, the phenomena of **partial coalescence** do not occur.
- Within the range of partial coalescence, the process can be divided into three regimes, depending on different forces, namely viscous force, surface tension force, inertia force and buoyancy force.
- **Partial coalescence** occurs in **liquid/ air medium** for very low velocity and as the velocity increases **complete coalescence** occurs.
- As the Weber number is increased, the phenomena which occurs are: **partial coalescence, complete coalescence, small thick jet (with or without secondary drop), thin jet, large bubble with thin jet, small bubble with thick jet, long thick jet.**
- The type of phenomena depends on the **direction of liquid flow** during **retraction stage**.

- Large bubble entrapment is observed in a wide region on the V -D map. The regime of large bubble entrapment on the **V -D map** and on the **We-Fr map** has been identied.
- The shape of the drop must be **prolate** at the time of impact for large bubble entrapment to take place. Sometimes the large bubble is accompanied by the entrapment of a small bubble.
- The **vortex ring** which is generated near the interface, later, pulls and curls-up the interface to form the **roll jet**. The roll jet merges at the central axis to entrap a large bubble inside the liquid pool. The **vorticity strength** must be strong enough to make the roll jet merge at the centreline, for the entrapment of large bubble.
- The emergence of **ejecta sheet** merged with the lamella, prevents the separation and penetration of the vortex ring onto the pool, which in turn, prevents the entrapment of large bubble.
- Within the large bubble entrapment regime, the enclosure depth, crater depth and pinch-off time decrease with the increase in impact velocity of the drops. The same parameters increase with the increase in size of the drops.

- B. Ray, G. Biswas and A. Sharma, Generation of secondary droplets in coalescence of a drop at a liquid/ liquid interface, ***Journal of Fluid Mechanics,*** Vol. 655, pp. 72-104, (2010)
- B. Ray, G. Biswas and A. Sharma, Bubble pinch-off and scaling during liquid drop impact on liquid pool, ***Physics of Fluids*****,** Vol. 24, pp. 082108-1 – 082108-11, (2012)
- B. Ray, G. Biswas and A. Sharma, Regimes during liquid drop impact on

a liquid pool, ***Journal of Fluid Mechanics***, Vol. 768, pp. 492-523, (2015).
- H. Deka, B. Ray, G. Biswas, A. Dalal, P. Tsai and A. B. Wang, The regime of large bubble entrapment during a single drop impact on a liquid pool. ***Physics of Fluids*** 29 (9),092101 (2017).

- Dr. Hiranya Deka (former PhD student, IIT Guwahati; currently with IFPEN, France)
- Dr. Pei-Hsun Tsai (National Taiwan University, Taiwan)
- Dr. Bahni Ray (former PhD student, IIT Kanpur; currently with IIT Delhi)
- Prof. Ashutosh Sharma (IIT Kanpur; Secretary DST)
- Dr. Amaresh Dalal (IIT Guwahati)
- Prof. Sam Welch (University of Colorado, USA)
- Prof. Stephane Zaleski (UPMC, France)
- Prof. An –Bang Wang (National Taiwan University, Taiwan)